




Research Article



A comparison of the spatial heterogeneities of surface fluxes simulated by INLAND model with observations at a valley and a nearby plateau stations in Central Amazon Forest

Elisângela Broedel^{1,2,6}  · Celso von Randow¹ · Luz Adriana Cuartas² · Prakki Satyamurty¹ · Alessandro Carioca de Araújo⁴ · Luiz Antônio Cândido³ · Javier Tomasella² · Antônio Donato Nobre¹ · Etienne Tourigny⁵

Received: 9 January 2022 / Accepted: 23 March 2022

Published online: 16 May 2022

© The Author(s) 2022 **OPEN**

Abstract

An improved version of the Integrated Land Surface Model (INLAND), incorporating the physical, ecological and hydrological parameters and processes pertaining to two subclasses of tropical forest in the central Amazon basin, a poorly drained flat plateau and a well-drained adjacent broad valley, is used to simulate the hydrological, energy and CO₂ fluxes. The model is forced with observed meteorological data. The experimental output data from the model runs are compared with observational data at the two locations. The seasonal variabilities of water table depth at the valley site and the soil moisture at the plateau site are satisfactorily simulated. The two locations exhibit large differences in energy, carbon and water fluxes, both in the simulations and in the observations. Results validate the INLAND model and indicate the need for incorporating sub-grid scale variability in the relief, soil type and vegetation type attributes to improve the representation of the Amazonian ecosystems in land-surface models.

Article Highlights

This manuscript draws attention to the spatial heterogeneity in Amazon forest mosaic and its effects on the ecosystem exchanges;

The inclusion of a lumped unconfined aquifer model is essential to simulate properly the water balance in the valley environment;

The results validate INLAND in a typical tropical forest ecosystem and indicate that previous works might have overestimated evapotranspiration.

Keywords Landscape heterogeneity · Topographic gradient · Land surface model · Energy and water balance · Carbon balance and central Amazon forest

Supplementary Information The online version contains supplementary material available at <https://doi.org/10.1007/s42452-022-05026-8>.

✉ Elisângela Broedel, elisabroedel@gmail.com | ¹Earth System Science Center, National Institute for Space Research (INPE), São José dos Campos, Brazil. ²Brazilian Center for Monitoring and Early Warning of Natural Disasters (CEMADEN), São José dos Campos, Brazil. ³National Institute for Amazonian Research (INPA), Manaus, Amazonas, Brazil. ⁴Brazilian Agricultural Research Corporation (EMBRAPA), Belém, Brazil. ⁵Barcelona Supercomputing Center (BSC), Barcelona, Spain. ⁶Brazilian Center for Monitoring and Early Warning of Natural Disasters (CEMADEN), Estrada Dr. Altino Bondensan, 500—Eugênio de Melo, São José dos Campos—São Paulo 12247-016, Brazil.



1 Introduction

An unperturbed patch of the Amazon forest appears homogeneous from the sky. In reality, the forest is a mosaic of landscapes with valleys, plateaus and slopes characterized by variable floristic compositions. At scales of the order of one kilometer, the characteristics of non-flooded tropical forest ecosystem, known as '*Terra Firme*', presents spatial variability of vegetation, soil type [1], topography [2], water fluxes [3] and phreatic zone depths and gradients [4]. The variabilities are masked by dense forest cover. The heterogeneity of landscape affects the exchange of radiation, energy, water and carbon between land and atmosphere. The exchange processes are fundamental to the functioning of the ecosystem [5] and to the regulation of evapotranspiration (ET) and carbon balance [6, 7].

In the central region of the Amazon forest, the landscape usually comprises plateaus, slopes and valleys. The plateaus are covered with high forest and are bounded by slopes, which descend into low-gradient valley floors [8]. The water table in the valleys is near the surface, for most of the year, with pools, puddles and small streams in some places, known as '*Igarapes*'. It is estimated that, in the central Amazon, plateaus, valleys and slopes occupy 31%, 29% and 40%, respectively, of the total surface area [8].

The Amazon forest environments are dynamic. Ground water from plateaus and slopes flows continuously down the slopes keeping the water table in the valleys near the surface even in dry seasons [9, 10]. The floristic composition of species, such as leaf area and root depth, over the topographic gradients, play an important role in energy and water budgets. In valley areas, the species are adapted to conditions of episodic hypoxia as indicated by the presence of adventitious surface roots and poorly drained hydromorphic sandy soils [11]. Such episodes induce a decrease in stomatal conductance and photosynthetic rate, limiting plant growth [12, 13]. In plateau areas, the water table is about 30 m below the surface [3, 4]. The extraction of water by vegetation occurs up to eight meters below surface, especially in dry season, to maintain high photosynthetic rates [14]. In these areas, the soil is extremely clayey ('Latosol') with high porosity, low water availability, and high-saturated hydraulic conductivity [15]. While surface runoff is dominant in the valley, the physical properties of soils and plants affect the infiltration process in the plateau, impacting the amount of water available in the soil for extraction by plant roots.

The representation of complex landscape is not included in the current and past Earth System

bio-geophysical models: BATS—Biosphere Atmosphere Transfer Scheme [16], SiB—Simple Biosphere [17], ISBA—Interactive Soil Biosphere Atmosphere model [18], CLASS—Canadian Land Surface Scheme [19], IBIS—Integrated Biosphere Simulator [20], CLM—Common Land Model [21], and JULE—Joint UK Land Environment Simulator [22]. These models consider tropical forest and its structure, as well as its functional characteristics, as being horizontally uniform, and thus a one-dimensional soil-vegetation column is sufficient for their description [23]. In order to characterize realistically the bio-geophysical processes, it is necessary that the models take into account the heterogeneities. For this purpose, it is important to better understand the differences between valley, slope and plateau in terms of water, energy and carbon budgets. The inability to account for these features may mask the real biosphere impact on climate functioning. A more accurate understanding of fine-scale spatial processes can lead to the development of more accurate parameterizations than those found so far.

Mathematical models with all the processes adequately included can play a crucial role in our ability to estimate the quantity of carbon that humanity can emit, in principle, to limit climate change and help the reduction of epistemic uncertainties in future climate scenarios and the changes in vegetation cover. This improves the comprehension of the impact of Amazon forest on global environmental change.

In spite of many modeling studies of the Amazon region, the mesoscale environments remain poorly explored. The present study aims to improve the understanding of the valley and plateau land surface fluxes. The objective of this work is to characterize and parameterize the landscape features (soil, vegetation and hydraulics) governed by relief attributes at local scale in a Land Surface Model, in order to simulate the differences in carbon, energy and hydrological fluxes between plateau and valley, at a central Amazon rainforest experimental site. In this paper, model results are compared with observational data. The following section describes details about the data and the methodology used in the work. Results and discussion are presented in Sect. 3. Section 4 draws some final considerations of the work.

2 Materials and methods

2.1 Study area description

The study area is an instrumented hydrological catchment of 6.37 km² (54° 58' W, 2° 51' S) located in the Cuieiras Biological Reserve (CBR). The site location is 80 km northwest

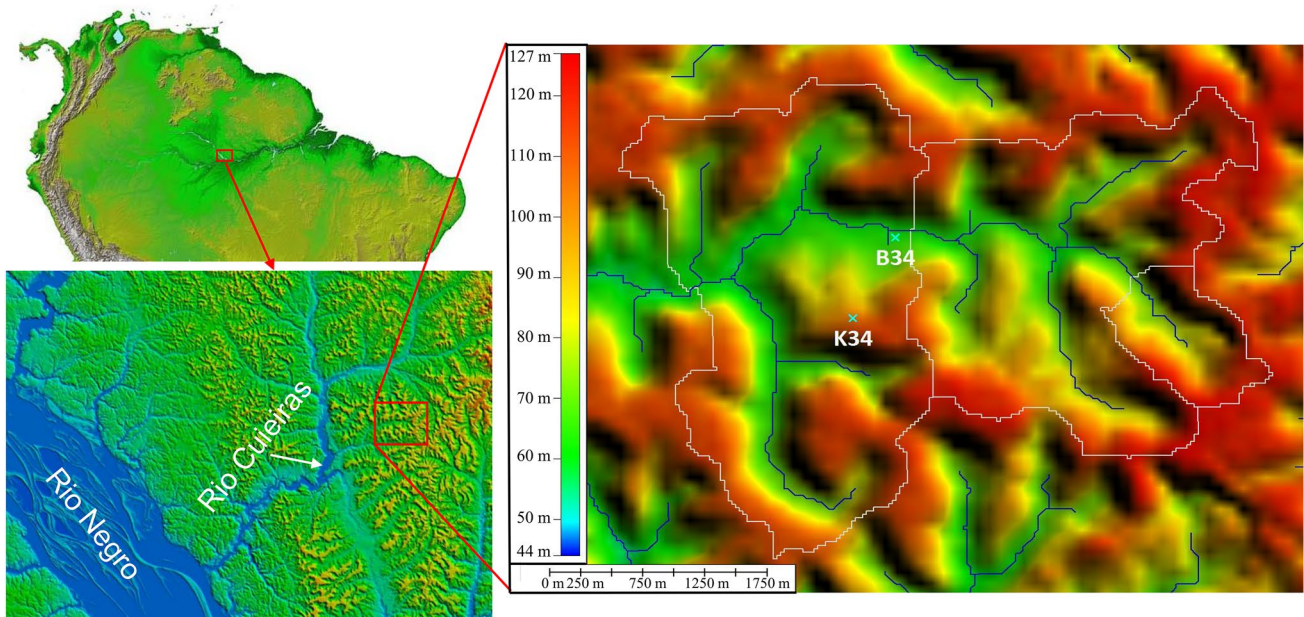


Fig. 1 Location of Cuieiras biological reserve, Manaus, Amazonas, Brazil. K34 and B34 points indicate the localization of the plateau and valley observation points, respectively

of Manaus within the pristine central Amazon tropical forest (Fig. 1). CBR presents a tropical rainforest climate (Af) according to Köppen classification [24]. Monthly average temperatures vary between 25 °C in July and 27 °C in November. Average relative humidity exceeds 80% any time of the year [25]. The annual rainfall varies from 1400 to 2800 mm with a climatological mean of approximately 2000 mm. The rainy season occurs between November and May and a relative dry season between June and October. This means that a rainy season is well defined, although temperature remains uniform and humidity remains high throughout the year. This seasonal variability is due to the South American monsoon variability and the annual migrations of the Intertropical Convergence Zone (ITCZ) and the equatorial trough.

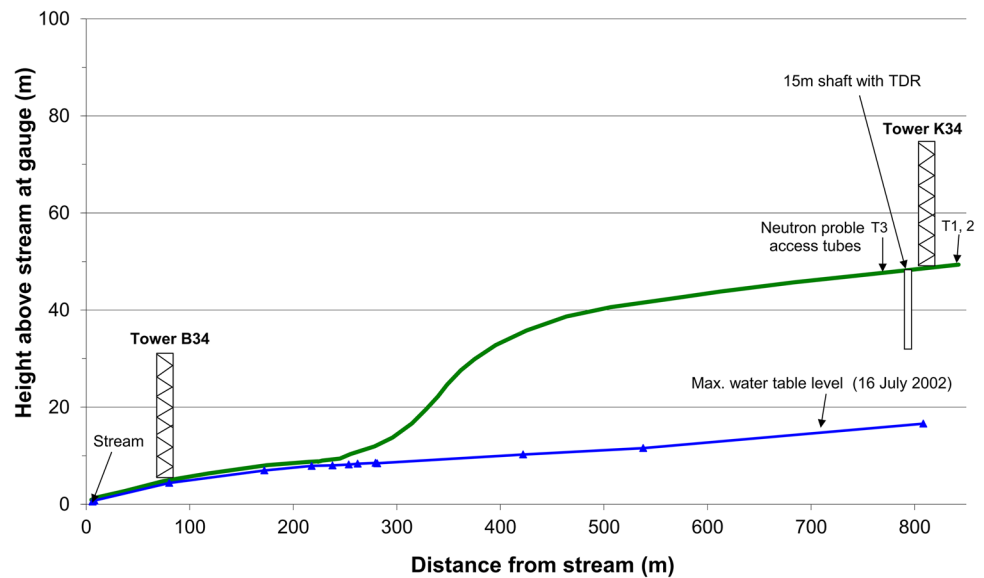
The site is a highly incised headwater catchment consisting of plateau areas that vary in height between 90 and 110 m above sea level (asl). The slopes are steep and concave, leading to broad and flat valley bottoms at 40–60 m asl. This topography is typical of the Amazon rainforest [8]. The vegetation cover on the plateau and slope areas is composed of tall and dense non-flooding tropical forest, with canopy heights varying between 30 and 44 m. In the valley, the ground-cover vegetation is less dense, with canopy heights varying from 15 to 25 m [26]. Soil composition can be classified into three dominant types along the topographic gradient: clayey Oxisols on the plateaus (Yellow Latosols in the Brazilian system), transitioning to less clayey Ultisols on the slopes (Podzol in the Brazilian system) and sandy Spodosols in the valley areas [27]. In

the valley, surface water table up to 100 m wide (swampy pools) is present yearlong. Detailed descriptions of the site can be found in other works [1, 2, 28–30]

2.2 Data sets

Meteorological and hydrological datasets used in this study are provided by the Large-Scale Biosphere–Atmosphere (LBA) Experiment in the Amazon. The local meteorological datasets come from two micrometeorological eddy flux towers located 600 m apart: one on the plateau (known as K34; 2° 36′ 32.67″ S, 60° 12′ 33.48″ W, 96 m asl), and the other on the valley bottom (known as B34; 2° 36′ 09.8″ S, 60° 12′ 44.5″ W, 42 m asl), with an elevation difference of 54 m (Fig. 2). The plateau tower provided the data for this study from January 2000 to December 2011, that includes air temperature (°C), precipitation (mm), downward shortwave and longwave radiation ($W m^{-2}$), relative humidity, carbon dioxide CO_2 ($\mu mol m^{-2} s^{-1}$), latent LE ($W m^{-2}$) and sensible H ($W m^{-2}$) heat fluxes, and wind speed ($m s^{-1}$). The valley bottom tower provided data from January 2006 to December 2006. All measurements were conducted just above the tower top with temporal resolution of 60 min. Details about measured variables and descriptions about K34 and B34 tower instrumentation are found in other studies [28, 31]. Lastly, the climatological monthly average precipitation was obtained from National Institute of Meteorology (INMET), for the city of Manaus, between 1901 and 1999.

Fig. 2 Topographical gradient at Cueiras site in central Amazon tropical rain forest (green line) and instrumentation. Blue triangle symbols show the height of the water table at the positions of boreholes for monitoring



The hydrological data collected from the plateau and valley areas includes soil water content ($\text{m}^3 \text{m}^{-3}$), stream discharge ($\text{m}^3 \text{s}^{-1}$) and water table level depth (m). The plateau soil water content data was obtained by neutron probes from three sampling access tubes T1, T2 and T3, schematically shown in Fig. 2, installed 4.8 m depth, on weekly or biweekly basis from December 2001 to December 2006 [4]. It was also obtained by Time Domain Reflectometry (TDR) via six sensors at varying depths (0.8–8.0 m) installed along 15 m shaft walls, recording data on hourly basis between January 2003 and February 2006 [14]. The water table depth and stream discharge data in the valley area are available for the period July 2002—October 2006. The stream discharge was measured using the ultrasonic Doppler technique every 30 min and downloaded on a weekly basis [2]. The water table depth was measured weekly via seven piezometers (Polyvinyl Chloride tubes with 5 cm diameter and filters) placed over the valley area [3].

2.3 The INLAND model and development of an unconfined aquifer model

The INtegrated LAND surface Brazilian model (INLAND) was developed based on IBIS model [20, 32]. INLAND included all the main features of IBIS, using a modular and physically consistent framework to perform integrated simulations of water, energy, and carbon fluxes. Some improvements were embedded into INLAND modules (INLAND, v1.0) to simulate tropical processes [33, 34].

Land surface module of INLAND is based on the second-generation LSX model [35] with six soil layers of varying thicknesses and with an upper (trees) and a lower (shrubs and grasses) canopies. There are twelve plant functional

types (PFTs), each with distinct carbon pools for leaves, stems and roots. The Amazon basin is represented by the tropical broadleaf evergreen tree PFT. INLAND model consists of three modules with their characteristic temporal scales: a land surface module (minutes to hours), a vegetation phenology module (days to weeks), and carbon balance and vegetation dynamics modules (yearlong). Here, we give a gist of the modules that are most relevant to this study.

Soil module simulates soil temperature, water content and ice content (when required) in each soil layer and solves the θ -based form of the Richard's equation, where the soil moisture change in time and space is a function of soil water retention curve, soil hydraulic conductivity, upper and lower boundary conditions and plant water uptake. The plant root-water uptake, represented by a sink term in the macroscopic Richard's equation, is a function of atmospheric demand, soil physical properties, root distribution, and soil moisture profile [32].

Drainage from the bottom soil layer is modeled assuming gravity drainage and neglects interactions with groundwater aquifers. The lower boundary condition for the drainage is set via an empirical coefficient ranging from 0 (no drainage) to 1 (100% free drainage). This methodology is applicable to plateau areas, where groundwater responses are more gradual due to longer water percolation time through a deep vadose zone. However, there is a clear limitation in the case of the valley areas, since baseflow is crucial to sustain discharge during the dry season. Moreover, there is a direct drainage dependence on the time-variation of the amount of water stored in the valley. Therefore, a lumped unconfined aquifer model [36, 37] was incorporated into INLAND, in order to represent the contrasting groundwater responses in both environments

and, at the same time, keeping the model's simplicity. The water table is interactively coupled to the soil column through the soil drainage fluxes (groundwater recharge), represented by the following water balance equation:

$$S_y \frac{dH}{dt} = I_{gw} - Q_{gw}, \quad (1)$$

where S_y (dimensionless) is the specific yield of the unconfined aquifer; H (mm) is the water table level above the datum; I_{gw} (mm day^{-1}) is the groundwater recharge flux, which is the flux at the interface of unsaturated and saturated zones (i.e., the water table); and, Q_{gw} (mm day^{-1}) is the groundwater discharge to streams (i.e., groundwater runoff). Central Amazon rainforest valley sandy soils have S_y about 0.265 [38].

A regression analysis was performed to obtain a (non-linear) relationship between the baseflow discharge and water table depth [36]. The regression data spanned over 5 years of baseflow discharge (Q_{gw}) and water table level (D_{gw}) for the valley study site. A strong relationship was identified (coefficient of determination $R^2 = 0.85$; Fig. 3). The baseflow flux was separated from the daily discharge using a digital recursive filter technique [39]. This method is widely used for the continuous partitioning of streamflow discharge between surface runoff and baseflow, since it is fast, efficient, reproducible and objective [36, 40–43].

The groundwater model represented by (1) and fitting line shown in Fig. 3 were interactively coupled with the soil model in INLAND. The total height of the active unsaturated soil column can vary in response to water table depth fluctuations because the number of unsaturated layers is variable [36].

The INLAND model includes a non-linear root water extraction scheme to describe the impact of soil water

stress [20]. The potential transpiration is first distributed over the entire rooted zone and, then, restricted to actual root water uptake by a soil water stress reduction function. A linear function was added to describe the soil water uptake reduction caused by root oxygen deficiency [44]. Under optimal moisture conditions, the maximum possible root water extraction rate, integrated over the rooting depth, is equal to the potential transpiration rate. Under non-optimal conditions (i.e. soil is either too dry or too wet), the root water extraction rate may be restricted, reducing transpiration. For saturated conditions, the reduction of root water uptake occurs between 0.83 and 1.0 degree of soil saturation, which leads to a reduction of 17–0% in the plant transpiration.

2.4 Simulations with INLAND Model for plateau and valley areas

Model simulations were run with the single-point offline version of the model (INLAND 1D) with the CO_2 concentration in the atmosphere set to a constant value of 400 parts per million (ppm). The simulations were performed at plateau and valley areas to determine the land surface fluxes near the observed data locations. The model was forced with observed hourly meteorological data collected at K34 tower for 12 full years, from January 1st, 2000, to December 31st, 2011. The initial 60 min of the simulation, considered tune up, was discarded from the analysis.

Initially, we considered the model parameters calibrated for a plateau area for the same study site [45]. However, this calibration was performed without emphasis on soil water dynamics processes. Parameters for the valley area, such as Leaf Area Index (LAI), canopy height and optical reflectance were modified based on observed data and the structural characteristics of vegetation [4, 46–50]. In order to determine fitting parameters of the water retention curves and hydraulic conductivity functions of a soil column for both areas, we used observed data and data from literature for the study site. The Oxisol hydraulic properties of plateau areas were taken from previous studies [15, 51, 52], since PedoTransfer Functions (PTFs) derived using data from temperate region soils do not accurately represent the properties of tropical soils [53]. Although Oxisols have high clay content, they have low water availability and high-saturated conductivity. These characteristics differ from temperate clay soil characteristics. In the case of hydraulic properties for sandy soils located in the valley area, we used the soil parameters recommended by preceding researches [54, 55].

The six soil layer thicknesses in INLAND, top to bottom were set to 0.20, 0.30, 0.50, 1.0, 2.0 and 4.0 m, for the plateau area. In the valley, the total soil depth was set to 4 m, with layer thicknesses of 0.10, 0.20, 0.30, 0.40, 1.0 and

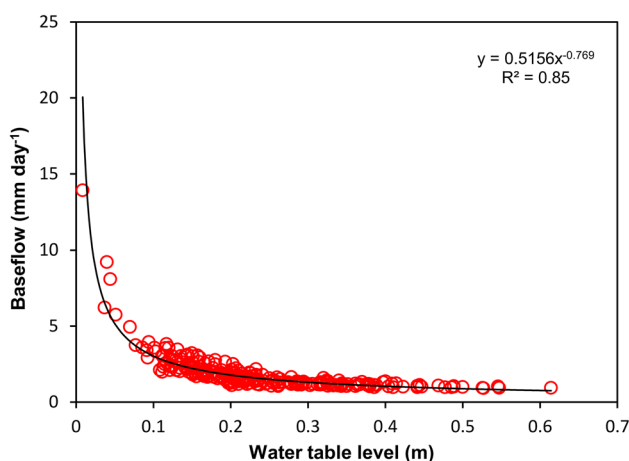


Fig. 3 Regression analysis between water table depth and baseflow data valley, from July 2002 to October 2006

2.0 m. The parameters of the INLAND model were fitted via trial and error, comparing simulations with the observational data from both plateau and valley areas, including the latent heat flux (LE), sensible heat flux (H), net radiation (R_n), net ecosystem exchange of CO_2 (NEE), soil moisture and water table level.

2.5 Balance equations and evaluation metrics

The simulated and observed energy and hydrological fluxes are based on the following balance equations:

$$R_n = H + LE + G \tag{2}$$

$$\Delta s / \Delta t = P - ET - R_{total} \tag{3}$$

where the net radiation R_n is the difference of shortwave solar radiation and the longwave terrestrial radiation, G is conduction of energy into the ground, and P is precipitation. LE is given by $\lambda \cdot ET$, with λ as latent heat of vaporization and ET as evapotranspiration. All the terms in (2) have

units of $J \cdot m^{-2} \cdot s^{-1}$. However, G is neglected, since it is much smaller than the other three components. The left hand side of (3) is the rate of change of storage of water (s) in the soil. Total runoff (R_{total}) is the sum of the surface runoff (R_s) and subsurface drainage (D). We note that P , ET and R_{total} are always equal or greater than zero.

Statistical metric bias, coefficient of determination (R^2), and the Root Mean Square Error ($RMSE$) are used to determine 'goodness-of-fit' and to check model performance [56].

3 Results and discussion

3.1 Water table dynamics and its simulation in the valley area

Since the water table at the plateau site remains deep, nearly 30 m, the model simulations with 6 m soil depth do not capture the water table depth (WTD) variability. Therefore, we discuss the WTD only at the valley site.

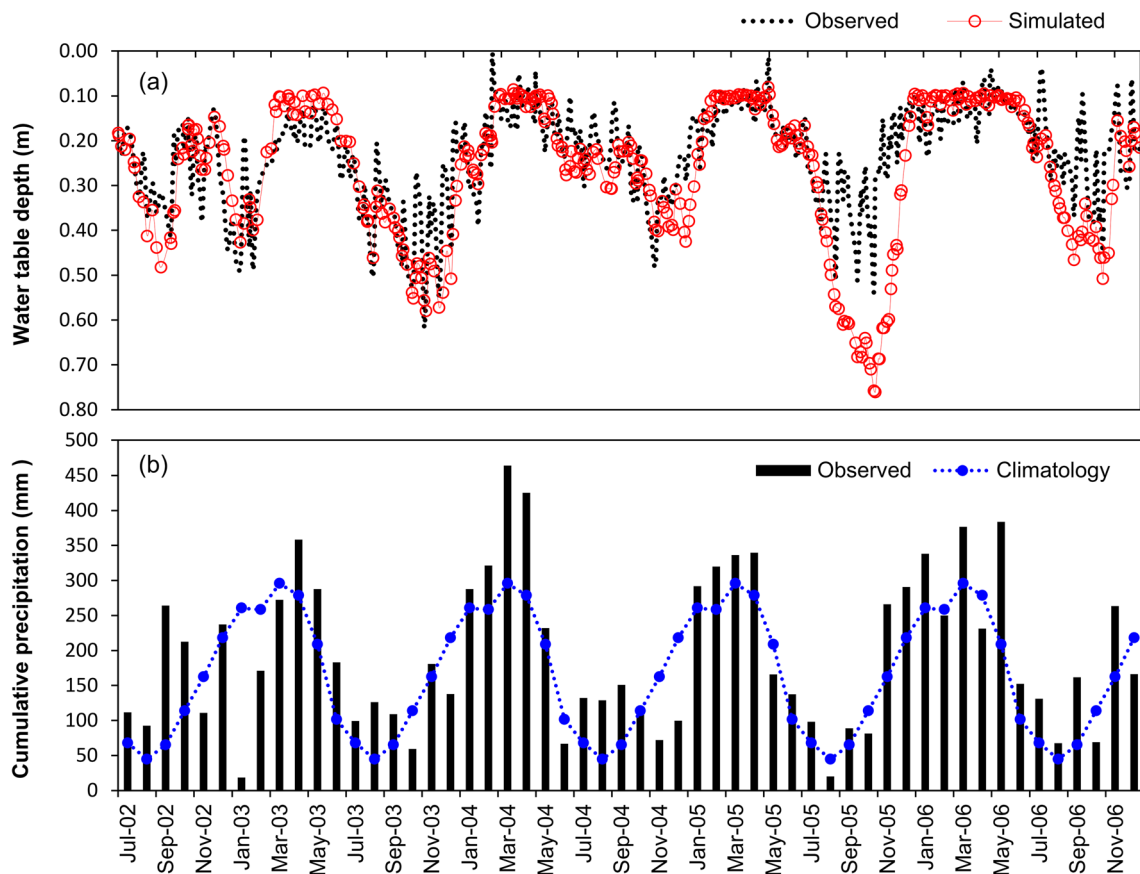


Fig. 4 **a** Observed and simulated water table depth fluctuations in the valley area, from July 2002 to December 2006. **b** Observed precipitation during the same period (vertical bars) and climatological

mean precipitation between 1901 and 1999 in the city of Manaus (dashed line)

The lumped unconfined aquifer model coupled to the INLAND model was able to predict the observed weekly values of WTD satisfactorily. Figure 4a shows the simulated and observed variations over the study period (2002–2006) in the valley environment. The WTD is the response to the observed precipitation at the study site shown in Fig. 4b. It can be seen that almost all months in the study period received rainfall in excess of their respective climatological values (blue line), except in two conspicuous drought events, January–March 2003 and November–December 2004 (Fig. 4b). Significant wet periods were April–September 2003, January–May 2004, January–April 2005 and May–September 2006. Heuristically, we employed the following criteria: a drought episode is a period of two or more consecutive months in which the rainfall is less than 50% of the climatological value. A wet event is a period of two or more consecutive months in which the accumulated precipitation exceed the climatological value by 30%.

The observed peaks and depressions in water table level (black dots in Fig. 4a) are respectively almost simultaneous with maxima and minima rainfall, as in September 2002, April 2003, March 2004, April 2005 and March 2006, January 2003, October 2003, October 2004, August 2005 and October 2006 (with the exception of July 2006). This occurs because surface or near-surface water table variations respond almost immediately to the precipitation variations. The rainfall data in the graph are monthly-accumulated values, while WTD values are weekly, and therefore lags of less than a month between rainfall and WTD can not be delineated.

In the post dry season of 2003, the water table fell below 0.61 m depth in November, although the rainfalls in the preceding months (April through September 2003) were systematically higher than climatological values. The steep fall in water table level can not be explained by the small negative anomaly observed in October 2003 rainfall. The fall may be attributed to reduction of drainage flow from upstream portion of the Amazon Basin. The model also simulated satisfactorily higher values of WTD in November 2003. More strikingly, in the 10-month wet period November 2005 through August 2006 the water table remained very near to the surface (above 0.25 m) and the simulation correctly followed this long event. On the whole, the seasonality seen in the observed WTD is also seen in its simulated values. However, the curve of the simulated values is somewhat smoother than the observed data curve. That is, the model does not predict abrupt changes. Furthermore, the model could not capture the zero and near zero WTD events in March 2004 and April 2005. The WTD is overestimated by the model during the period September–November 2005. In spite of these minor deficiencies, the INLAND model adequately

Table 1 Performance of INLAND model in representing the depth of the water table in the valley located in the study area during the period 2002–2006

	Water table depth (m)		
	Bias	RMSE	R ²
Wet season 2002–2003	−0.05	0.08	0.65
Wet season 2003–2004	0.03	0.09	0.68
Wet season 2004–2005	0.01	0.07	0.71
Wet season 2005–2006	0.07	0.18	0.52
Total mean	0.02	0.11	0.64
Dry season 2002	0.04	0.07	0.66
Dry season 2003	−0.03	0.06	0.79
Dry season 2004	0.01	0.04	0.57
Dry season 2005	0.11	0.18	0.52
Dry season 2006	0.07	0.10	0.58
Total mean	0.05	0.09	0.62

simulated the transitions between wet and dry conditions, showing reasonable agreement with observations. Statistical comparisons between the simulations and the observations are given in Table 1. The mean RMSE is 0.11 m with $R^2 = 0.65$ in the wet seasons, while it is 0.12 m with $R^2 = 0.62$ in the dry seasons. The observed and simulated mean WTDs for the whole period were, respectively, 0.21 and 0.22 m, during the rainy season (November–May), increasing to a depth of 0.26 and 0.31 m, respectively, in the dry season (June–October).

The INLAND simulations during 2002–2006 presented here were more representative than the CLM results reported by previous work [57]. Simulations with the Distributed Hydrology Soil Vegetation Model (DHSVM), at the same site, also produced higher standard deviation ($RMSE = 0.25$ m) during both wet and dry seasons (2002–2006), with an R^2 of 0.60 and 0.72 for the wet and dry seasons, respectively [4].

3.2 Soil moisture variability in the plateau area

Soil moisture variations in the valley are not discussed because the soil in the valley remained always saturated at all considered depths.

The observed and simulated soil moisture variations at the plateau site in the six layers during the 6-year period 2001–2006 are shown in Fig. 5. First, we observe that the model simulations with default values for the hydrological and vegetation parameters (gray line) are far from the observed values at the site (black dots). Moreover, the simulated values with parameters adjusted to tropical forest conditions (red) show good agreement with both magnitude and seasonal variability in the observations, at all depths. Although the temporal frequency of observational

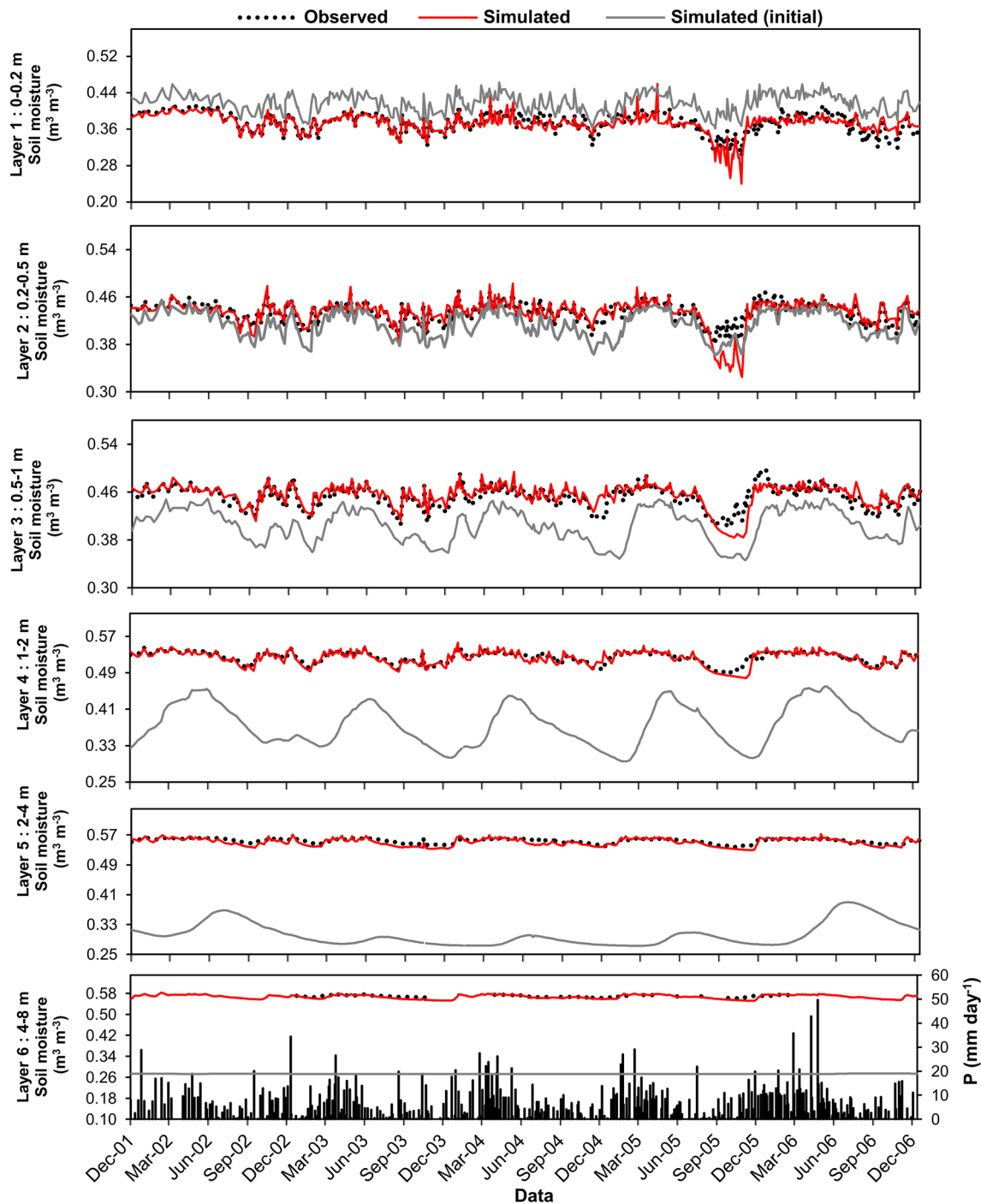


Fig. 5 Observed and simulated soil moisture results for the six layers in the plateau. Observational data have a weekly or biweekly temporal frequency. Layers 1–5: from December 2001 to December

2006, obtained from neutron sonde. Layer 6: from January 2003 to February 2006, obtained from TDR. The grey line represents the soil moisture values considering default parameters of the model

data for the deepest layer was hourly, weekly averages are shown in the graph to match the observational data from the first five layers (obtained by neutron probe) from January 2003 to February 2006.

In the initial experimental setup, soil parameter values from the existing literature were utilized in the model

run [15, 51, 52]. Further analyses demonstrated that three of the six soil parameters (Table S1, in supplementary material) were sensitive to a default setup: porosity (*poros*), Campbell’s parameter (*bex*) and hydraulic conductivity (*hydraul*) [14]. Tuning of these parameters was

crucial for matching simulated soil moisture profiles with observations.

The simulated soil moisture content presents an annual cycle, with decreasing amplitude in the deeper layers. In the first four soil layers, the differences between dry and wet seasons were more pronounced compared to other layers. This behavior is related to a quick precipitation response in the topsoil layers and to their high macro porosity. At greater depths, the response to rain events is damped, particularly in the deepest two layers, which respond slowly to the seasonal precipitation variability.

In general, the model slightly underestimated the soil moisture content and presented an $RMSE$ of $0.017 \text{ m}^3 \text{ m}^{-3}$ with R^2 of 0.54 for the first layer, and $RMSE$ of $0.006 \text{ m}^3 \text{ m}^{-3}$ with R^2 of 0.71 for the sixth layer (Table 2). The $RMSE$ decreased with depth because the temporal variability of moisture in deep soils is very small. The reason is due to high micro porosity and low permeability responsible for slow percolation at deeper layers [58]. Very small soil moisture variation in the last two layers on the seasonal scale indicates very little presence of roots and water availability for plants at these depths, as observed in previous work [59]. Therefore, these layers exhibit very little sensitivity to intra-seasonal, as well as seasonal variations in precipitation. The results indicate no significant water extraction from roots at these depths because there was

sufficient water in the layers above 400 cm during most of the year [14]. For example, the sixth layer (depth of 4–8 m) had a nearly constant water content of $0.57 \text{ m}^3 \text{ m}^{-3}$. The R^2 increased from the surface up to 2 m depth and then decreased. The model is unable to deal properly with minuscule variations in soil moisture at deeper layers.

A notable feature observed in the simulation results is the underestimation of soil moisture in the post dry season of 2005 (Sep–Dec) in the layers above 1 m. The observed data also indicated pronounced depletion of soil moisture during this period, perhaps due to more intense root uptake than normal. Differences in the water content at the end of the dry season of 2005 between the observational and simulated results could be due to differences in the actual versus assumed root distributions.

3.3 Water fluxes in the plateau and valley areas

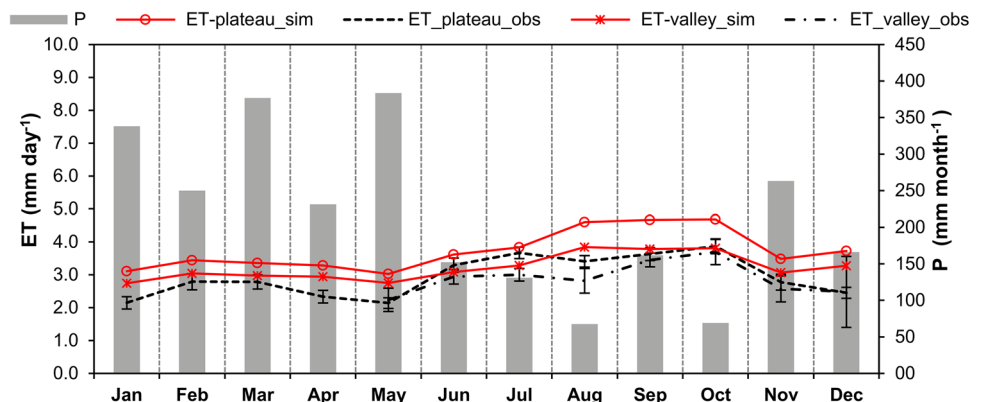
3.3.1 Evapotranspiration

The identification and improvement of soil physical parameters for soil water dynamic simulation in a tropical forest had a positive impact on the modeling of surface fluxes, mainly on ET flux [14]. However, Amazon basin studies lack investigations of the soil physical parameters, mainly at deeper levels, and the climate models are forced to consider shallow and homogeneous soil. The inclusion of the most representative vegetation and soil parameter sets for plateau and valley forests (Table S1), along with the incorporation of the unconfined aquifer model into the INLAND model for the representation of water fluxes in valleys, allowed to simulate the differences in ET fluxes between the plateau and the valley satisfactorily (Fig. 6). First, we notice that the observed values in the rainy period, December through May, are equal in both locations. In the dry season, June through November, the plateau transpires more than the valley because the vegetation over the plateau is denser and the incoming solar radiation is larger. Its ET varies between 2.4 mm day^{-1} in

Table 2 The $RMSE$, bias and R^2 calculated from weekly or biweekly soil moisture data

Layer (m)	N°	$RMSE$ ($\text{m}^3 \text{ m}^{-3}$)	Bias ($\text{m}^3 \text{ m}^{-3}$)	R^2 –
0.0–0.2	1	0.017	–0.004	0.54
0.2–0.5	2	0.14	–0.001	0.65
0.5–1.0	3	0.012	0.003	0.70
1.0–2.0	4	0.008	–0.002	0.79
2.0–4.0	5	0.007	–0.004	0.72
14.0–8.0	6	0.006	–0.003	0.71

Fig. 6 Mean monthly observed precipitation in the study area (P) and total evaporation (ET) simulated and observed in the plateau and valley areas, during 2006



December to 3.1 mm day^{-1} in July. Higher values of dry season transpiration are sustained by deep root water intake.

The annual mean simulated ET on the plateau is 3.7 mm day^{-1} , higher than 3.2 mm day^{-1} in the valley. In both places, simulated values are close to their respective observed values (plateau = 3.0 mm day^{-1} ; valley = 2.9 mm day^{-1}), which is in agreement with values reported in the literature, 3.8 mm day^{-1} on the plateau and 3.6 mm day^{-1} in the valley [9, 60]. The extraction of water from soil when water table is near surface is 0.5 to 1 mm day^{-1} , while its value is approximately 3 mm day^{-1} when the water table is below 1 m depth. This is because surface water is used for evapotranspiration when available [9]. In general, the graphs show systematic overestimation in the simulations in all seasons. However, the seasonal variability is reproduced in the simulations. The ET overestimation over the plateau is larger by nearly 0.5 mm day^{-1} . One interesting aspect is that the variability of monthly rainfall in a given season does not influence ET , as seen in Fig. 6. Then, vegetation density and solar radiation, instead of water availability, determine ET in the Amazon forest.

A possible explanation for the discrepancies in the results could be related to the lack of closure of the energy balance, a well-recognized problem of the eddy covariance method [61, 62] that was already reported by other studies in Amazonia [63–66]. The infrared gas analyzer (IRGA-LI-COR, model LI-7500) used to obtain LE is not reliable during rainy periods due to failure of the instruments caused by water drops standing over the sensors heads [67, 68]. Therefore, potential interference of rainfall can also be responsible for underestimation of LE in the study area, in both plateau and valley.

Mean ET over the year of 2006 corresponded to 55.7% of precipitation in the plateau and 45.4% in valley areas. Out of the total loss by ET , 76% were due to transpiration, at both sites. This percentage is higher than 53% found by previous work (same site) during the period from 2001 to 2004 [3] and the value of 56.9% obtained using the hydrological model DHSVM [4]. Higher ET percentage means that lesser part of precipitation is available for runoff and infiltration, according to (3). This indicates that the year 2006 was atypical.

The observed evaporation of the intercepted water (interception loss) represented 21.2% and 19.2% annually in the plateau and valley regions, respectively, while 2.5% and 3.8% were associated with direct evaporation from the soil in the plateau and valley, respectively. The direct evaporation is small because the surface atmospheric layer under the canopy is near saturation. Intercepted water simulated by INLAND during the wet season of 2002/2003 corresponded to 21.3% of ET in the plateau area, close to

the observations of 21.4% [29]. The water interception by the valley canopy was slightly lower than over the plateau, while soil evaporation was about 52% higher than over the plateau. These results reflect lesser tree density [46], lower and a more open canopy [47, 48], lower LAI [4] and a tree composition with less species [49, 50], when compared to the plateau.

3.3.2 Surface runoff and deep drainage

The observations of surface runoff (R_s) and deep drainage (D) are for the whole CBR area and include contributions of plateau and valley areas, while the same flows simulated by INLAND are obtained for the valley and the plateau sites separately. The weighted mean of the valley and the plateau values are compared with the observations to assess model performance. The weights used are their respective fractional areas: 0.569 in plateau and 0.431 in valley [8].

Figures 7a and b show monthly means of the simulated surface runoffs and subsurface drainages, respectively, at the valley and plateau sites, along with the observed values for the whole CBR from 2002 to 2006. Runoff (Fig. 7a) and drainage (Fig. 7b) did not vary much during the relative dry period July through November. However, in the wet period they gradually increased from December to April, attaining observed peak values in the month of April when the region received the largest mean monthly rainfall of nearly 360 mm (equivalent to 12 mm day^{-1} on the average). The preceding month of March also received almost an equal amount of rainfall. It can also be seen immediately that the runoff is less than the drainage during both wet and dry periods.

For argument's sake, here we make a heuristic analysis considering reasonable estimates of the components of hydrological balance Eq. (3) for the month of April. The mean runoff (Fig. 7a) and drainage (Fig. 7b) were in excess of roughly 2 mm day^{-1} and 4 mm day^{-1} , respectively, resulting about 6.5 mm day^{-1} . From Fig. 6, ET is estimated as 2.5 mm day^{-1} . The difference ($P - R_s - D - ET$) of nearly 3 mm day^{-1} went into storage (accumulation in the soil and in the aquifer), which was used in the upcoming dry period, mostly for evapotranspiration.

Figure 7a and b also show that observed mean monthly D is higher than R_s in the period 2002 through 2006 (black lines), in all months. This characteristic is reproduced in the model simulations (blue lines). However, the simulated surface runoff and drainage values are higher than corresponding observed values in the rainy season and lower than observed values in the dry season, resulting in a higher amplitude of the seasonal variability by the model. Although the 0–8 m layer is sufficient to simulate ET and carbon assimilation [3, 14], a significant portion of the water transfer by free drainage from the unsaturated

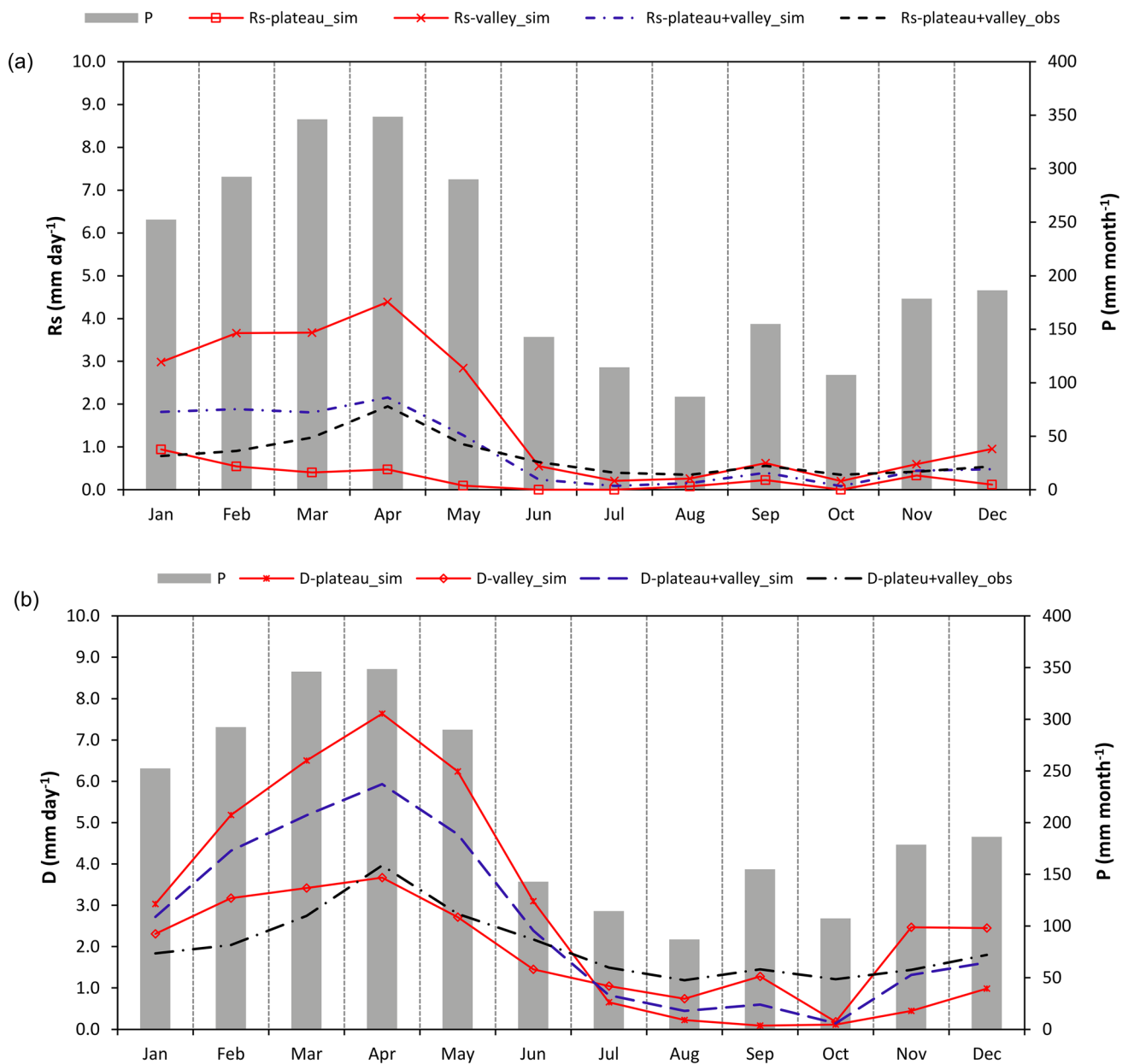


Fig. 7 **a** 5-Year mean surface runoff (R_s) simulated (blue) and observed (black) in plateau and valley from 2002 to 2006; **b** Same as in (a) except for groundwater drainage (D). Mean monthly observed precipitation in the study area (P) refers from 2002 to 2006

zone to the aquifer has not been taking into account. This reduces the efficiency of the model in representing the partitioning between vertical drainage and runoff.

Observed data runoff values are not available for each site separately. However, previous studies showed that over the plateau area, R_s is very low or even absent because the main mechanism of runoff generation is saturation overland flow [3, 69]. Simulated R_s in the plateau area presented an average of 3.9% of total precipitation, during 2002 to 2006, because the runoff is either very small or absent during the 6-months period July to

December, which is in agreement with other studies in different regions of the Amazon Basin [70–72]. In the valley area, however, R_s simulated by INLAND represented a higher fraction of precipitation when compared to plateau, about 25.3%. Simulated deep drainage is dominant in plateau area and is related with precipitation. A well-defined seasonal cycle is depicted, with higher values during the wet season (Fig. 7b), when the water table in the plateau is located about 35 m deep [3, 4]. D values represent a large fraction of the total precipitation, corresponding to 41.3% and 27.2% in the plateau and the valley areas,

respectively, similar to the values estimated previously for the same area [14].

Total simulated D flux (plateau + valley) was 3.7 mm day^{-1} and 0.9 mm day^{-1} during wet and dry seasons, respectively, while observations indicate 2.4 mm day^{-1} in the wet season and 1.5 mm day^{-1} in the dry season. In general, INLAND model overestimated D during the wet season (bias = 1.3 mm day^{-1}) and underestimated in the dry season (bias = -0.6 mm day^{-1}). A likely explanation for these seasonal discrepancies are related to the fact that simulated D did not consider the slow travel time of the horizontal water transfer from the saturated zone of the plateau to the valley bottom, which is responsible for the seasonal time-scale basin response delay. It is estimated that the average transfer time is about 3 months, highlighting the reduction of D in dry season [3]. The $RMSE$ was 1.7 mm day^{-1} and 0.8 mm day^{-1} in wet and dry seasons, respectively, suggesting a better model performance during wet season. There is an increase in the value of R^2 from wet to dry season. The results showed an overestimation of the total runoff during wet season (bias = 0.4 mm day^{-1})—mainly in the first months of the year when the precipitation is higher, and underestimation in the dry season (bias = -0.3 mm day^{-1}). During the wet season, the $RMSE$ was 0.6 mm day^{-1} and R^2 was 0.60. In the dry season $RMSE$ reduced to 0.3 mm day^{-1} and the correlation between the simulated and observed values, R^2 , decreased to 0.53.

Simulated discharge or total runoff (R_{total}) averages during the period from 2002 to 2006 represented 45.2% and 52.5% of the total precipitation, for plateau and valley areas, respectively. The lower percentage of R_{total} in relation to precipitation in the plateau is due to the higher ET in this area when compared to the valley. The mean values of R_{total} in relation to precipitation found in this study, in both areas, showed a close agreement with the values of 44.3% during the period from 2001 to 2004 [3], and of 49.3% obtained between 2000 and 2008 [14]. In addition, our results also corroborated the previously results obtained from 2002 to 2004 using the DHSVM model,

which stated that the total runoff represented 47.5% of the total precipitation in the plateau [3].

The INLAND performance metrics for ET , R_s and D discussed above are summarized in Table 3.

3.4 Energy fluxes

Observations and simulations of the diurnal evolution of net radiation (R_n) in the wet and dry seasons are shown in Fig. 8a and b, respectively. We observe that net radiation in dry season (Fig. 8b) is positive from 07 to 17 Local Time (LT) and peaks around 11 LT to nearly 600 W m^{-2} at both valley and plateau sites. From 17 LT in the afternoon to 07 LT in the morning, the forest loses energy (R_n is negative), with a slow rate of 30 W m^{-2} . The simulations (in red) properly follow the observations.

In the wet period, there is a dip around 50 W m^{-2} in the net radiation at 11 LT from about 500 W m^{-2} at 10 LT, in the valley site. This is probably due to cloud formation in the valley by the combined effect of downslope wind convergence and radiative heating. At 12 noon, the net radiation regains its intensity. However, there is no dip in R_n over the plateau exposed to solar radiation, meaning that the sky over the plateau remains mostly clear at this time of the day.

The simulations did not capture the late forenoon reduction in R_n in the valley. Although INLAND model takes into account the prescribed meteorological conditions, it is not capable to produce the convergent movements of surface air and the resulting cloud or fog formation. Moreover, the R_n simulated during daytime in the wet period (red lines in Fig. 8a), especially from 09 to 15 LT, was underestimated in comparison with observations at both valley and plateau site. Table 4 shows that the R^2 of the R_n simulations was 0.99 at the plateau in both seasons with $RMSE$ about 11.5 W m^{-2} and negative bias not greater than 4.3 W m^{-2} . At the valley site, bias was positive and $RMSE$ was of the order of 50 W m^{-2} in the wet season and 33 W m^{-2} in the dry season. The R^2 was over 0.95 in both seasons.

Table 3 The INLAND model performance for the representation of total evaporation (ET) during 2006; surface runoff (R_s) and deep drainage (D) during 2002–2006, from hourly data

	Wet season							Dry season				
	Flux	Year	Obs (mm day ⁻¹)	Sim	RMSE (mm day ⁻¹)	Bias	R ²	Obs (mm day ⁻¹)	Sim	RMSE (mm day ⁻¹)	Vies	R ²
Plateau	ET	2006	2.5	3.3	1.1	0.9	0.71	3.6	4.3	1.0	0.7	0.64
Valley	ET	2006	2.4	3.0	1.1	0.2	0.63	3.2	3.6	0.8	0.4	0.56
Plateau + valley	s	2002–2006	1.2	1.6	0.6	0.4	0.60	0.6	0.3	0.3	-0.3	0.53
Plateau + valley	D	2002–2006	2.4	3.7	1.7	1.3	0.79	1.5	0.9	0.8	-0.6	0.97

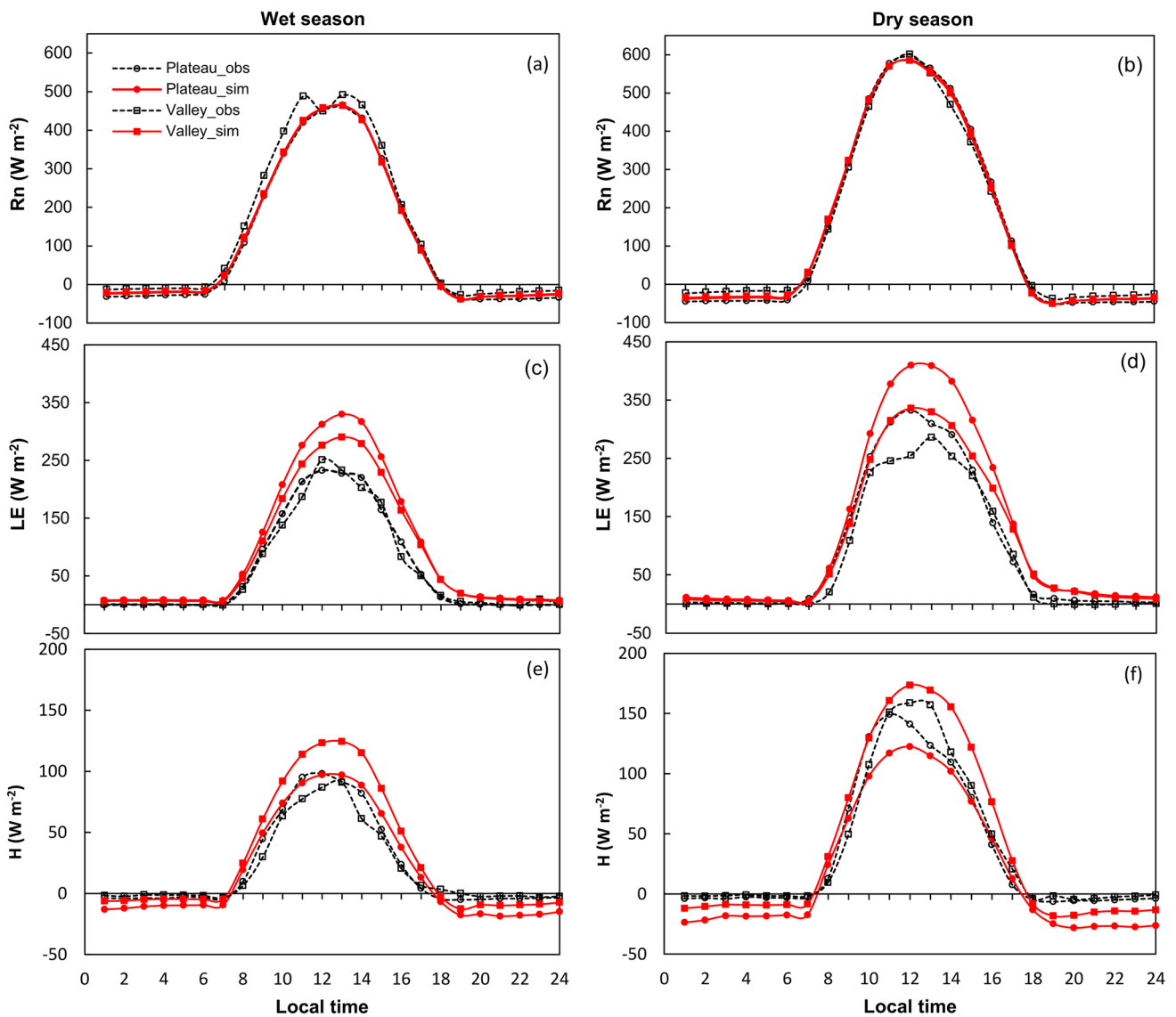


Fig. 8 Mean hourly observed and modeled energy fluxes in the wet and dry seasons of 2006

Table 4 RMSE, bias and R^2 calculated for the hourly energy fluxes

		Wet season			Dry season		
		RMSE ($W m^{-2}$)	Bias ($W m^{-2}$)	R^2 -	RMSE ($W m^{-2}$)	Bias ($W m^{-2}$)	R^2 -
Plateau	Rn	11.7	-4.3	0.99	11.3	-2.2	0.99
	LE	63.8	-34.0	0.85	66.8	-32.6	0.88
	H	26.4	2.8	0.75	33.4	14.2	0.78
Valley	Rn	44.7	15.0	0.97	29.8	10.8	0.99
	LE	63.6	-16.5	0.72	59.6	-20.8	0.81
	H	34.3	-11.0	0.66	34.9	-2.0	0.78

The constant-value albedo simulated by INLAND in the valley was 10.5% in the wet season and 10.8% in the dry season. These values were about 4% higher than previous

observational values [31, 73]. Furthermore, this difference could be due to the lower incoming longwave radiation, which is derived from meteorological data input in the

model, in the plateau. Observed incoming longwave radiation is consistently higher on the valley than on the plateau [31]. The INLAND model simulated the albedo differences in both areas, showing higher values on the plateau, like 12% in the wet season and 12.3% in the dry season, in fair agreement with observed data (wet season = 11%; dry season = 12%) [31, 73]. In order to simulate such differences, reflectance of near infrared radiation from leaves represented by the parameter *rhoevg_NIR* was adjusted to 0.31 and 0.26 for the plateau and valley, respectively (Table S1). The albedo difference between the two areas is due to the vegetation canopy structure [74]. In the plateau area, for example, the vegetation is denser, which favors a greater homogeneity of the vegetation, resulting in a greater reflectivity of the solar radiation. The seasonality of albedo also was correctly represented by INLAND, with higher values during the dry season. The forest canopy is darker during the rainy season due to greater radiation absorption by water, lowering the albedo [75].

The model was able to properly simulate the partitioning of available energy (R_n) with higher percentage used for *LE* (Fig. 8c, d) than for *H* (Fig. 8e, f), as verified in previous works [28, 63, 64]. Reasonable agreement between simulated and observed energy fluxes highlights an adequate model performance after the inclusion of improved vegetation and soil parameters (Table S1) and water table algorithm for the valley area. The *LE* annual averages corresponded to 84.9% of R_n , for the plateau, and 72.9% and for the valley, while *H* annual averages is 14.8% of R_n and 26.5%, respectively. These results are different from observed values, where *LE* is 60.4% of R_n for the plateau and is 50% of R_n for the valley. This shows that the *LE* flux is overestimated by the model. It can be noted in Fig. 6, which shows consistent overestimation of *ET* in all months compared to observations.

The simulated *LE* was higher for the plateau than for the valley, particularly in the dry season, agreeing with observed data. This difference is due to the higher simulated LAI on the plateau ($6.1 \text{ m}^2 \text{ m}^{-2}$) than in the valley ($5.8 \text{ m}^2 \text{ m}^{-2}$), which resulted in a higher evapotranspiration rate. Another possible reason is the excess water in the valley soils, which can produce oxygen-deficient roots and affect plant survival and functioning [76]. The overestimation of *LE* flux was higher on the plateau, where we found an *RMSE* of 63.8 W m^{-2} and R^2 of 0.85 in the wet season and an *RMSE* of 66.8 W m^{-2} and R^2 of 0.88 in the dry season (Table 4). The INLAND model was able to reproduce the seasonality of *LE*, showing higher values during the dry season for both areas (plateau = 124.6 W m^{-2} ; valley = 103.6 W m^{-2}), when compared to the wet season (plateau = 97.2 W m^{-2} ; valley = 86.3 W m^{-2}), which is in agreement with observed data.

In contrast, the simulated *H* fluxes (Fig. 8e, f) are higher for the valley area than over the plateau, in both wet (valley = 29.8 W m^{-2} ; plateau = 18.6 W m^{-2}) and dry (valley = 39.8 W m^{-2} ; plateau = 19.5 W m^{-2}) seasons, suggesting that more R_n was used to heat this environment. This behavior is in agreement with the observed *H* fluxes, mainly during the dry season (valley = 36.7 W m^{-2} ; plateau = 33.6 W m^{-2}), indicating a good performance of INLAND. The diurnal cycle also reveals that the seasonality of the *H* flux was consistently reproduced by the model, presenting higher values during the dry season in both areas, again in agreement with observed data.

The higher values of *H* in the valley compared to the plateau also show a significant bias in the simulated values of *H* for the valley. The model overestimated the observed hourly totals by 11% and 2% during the dry ($R^2 = 0.78$; *RMSE* = 34.9 W m^{-2}) and wet ($R^2 = 0.66$; *RMSE* = 34.3 W m^{-2}) seasons, respectively. This overestimation in the *H* flux was related to one of the most relevant *H* simulation parameters, *rhoevg_NIR* [77]. The vegetation-to-air sensible heat flux is a function of the leaf and stem temperatures. These two variables depend on solar radiation absorbed by the canopy and soil, and on the net absorbed fluxes of infrared radiation.

3.5 Net ecosystem exchange

Figure 9 shows the diurnal variations of the *NEE* fluxes simulated by the INLAND model and observations at the two sites, valley and plateau, for the wet season and the dry season of the year 2006. First, we note that the observations (black graphs) show larger negative diurnal peak values at the plateau site than at the valley site, which is attributed to higher density of vegetation. The peak in *NEE* over the plateau occurs at 11 LT in the wet season and 1 h earlier in the dry season. Another important observation is that *NEE* faces a reduction in flux between 11 and 12 LT in the wet season in the valley (Fig. 9a). This is caused by the dip in the net radiation (Fig. 8a), which is caused by reduced solar radiation due to clouding in the valley at those hours. Further exams over the observational data reveals that the nighttime positive values (respiration) continue up to 08 LT (early morning hours) in both seasons and remain negative (photosynthesis) up to 17 LT. The respiration rates during the night remain almost constant.

In general, the simulated daytime and nighttime *NEE* flux patterns follow satisfactorily the observed patterns. However, there are significant differences. The simulated daytime negative peaks are less sharp in both seasons. The wet season noontime dip in *NEE* in the valley is not reproduced. Once again, this is because INLAND model does not produce changes in atmospheric flow dynamics

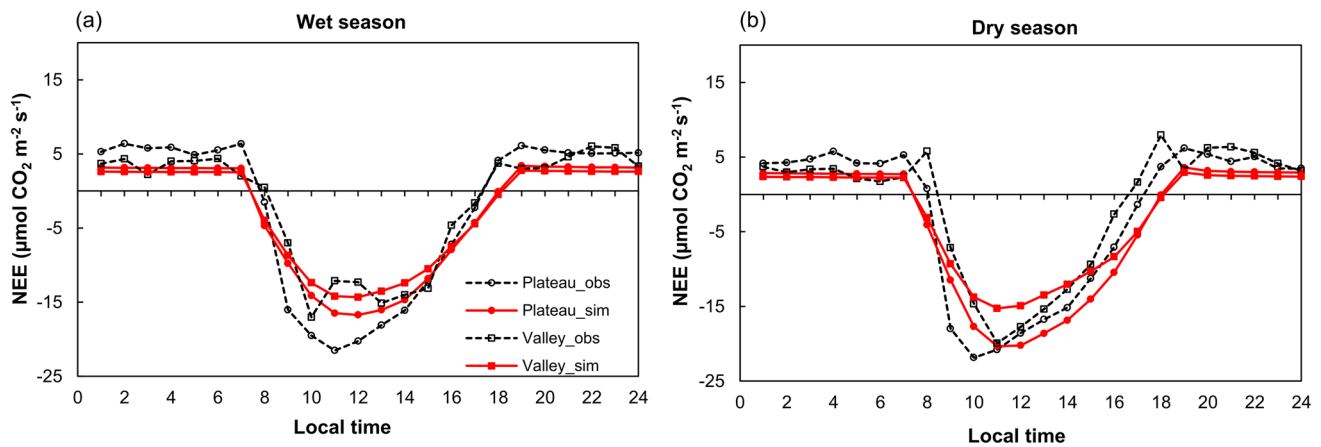


Fig. 9 Observed and simulated diurnal variation of net ecosystem exchange (*NEE*) rates between the forest and the atmosphere. Negative values (daytime) represent uptake of CO₂ from the atmosphere

(photosynthetic activity is higher than respiration). Positive fluxes (nighttime) are associated with emissions of CO₂ from the forest to the atmosphere (respiration activity only)

and formation of clouds. The nighttime *NEE* fluxes are also smaller than their corresponding observed values.

However, INLAND properly captured the difference between the two areas due to fine-tuning of vegetation and soil parameters at the plateau and the valley sites (Fig. 9a, b). Adjustments in photosynthesis parameters (Table S1) were essential to reduce the bias between simulated and observed *NEE* values. The daytime negative peak of *NEE* is placed 1 h later than in the observation in the dry season by the model. These differences show that the INLAND model needs further fine tuning to fit the tropical forest characteristics and should be run in dynamic mode, i.e., in conjunction with the diurnal changes in atmospheric flow. The discrepancy in the nighttime respiration intensity seems to be due to constant values attributed which can be seen in the horizontality of the graphs of the simulated values.

During daytime (photosynthesis-dominated processes), the simulated *NEE* fluxes over the plateau were higher than in the valley, in both wet and dry seasons, agreeing with observed data. The average *NEE* flux simulated during daytime on the plateau was

$-8.5 \mu\text{mol m}^{-2} \text{s}^{-1}$ and $-10.2 \mu\text{mol m}^{-2} \text{s}^{-1}$ in the wet and dry seasons, respectively (Table 5). In the valley, simulated *NEE* values were smaller by, approximately, 11.8% and 23.5% than the values over the plateau, for the wet and dry seasons, respectively. The higher *NEE* flux rate during daytime on the plateau suggests a stronger CO₂ uptake rate due to increased photosynthetic activity from a higher biomass yield in this area [78]. In addition, it was found that the biomass variation between plateau and valley is mainly associated with nitrogen availability [79]. The plateau area soil and plant leaves have a greater amount of nitrogen than in the valley, indicating a larger nutrient availability for biomass growth in the plateau [1]. It was conducted a 3 year long litterfall experiment in an area of 10 km² to the northwest of the present study site and measured a 3-year average yield of 8.3 tons C ha⁻¹ of litter in the plateau, and 7.4 tons C ha⁻¹ in the valley [69]. These results indicated that yield is greater over the plateau than in the valley. In addition, using sapflow data for the study site [80], it was showed that photosynthesis starts later and ends earlier in the valley area,

Table 5 Average observed and simulated net ecosystem exchange (*NEE*) values for plateau and valley during the day (06:00–18:00 h), night (18:00–06:00 h) and daily totals. The daytime peak observed and simulated is also includes

	Wet season $\mu\text{molCO}_2\text{m}^{-2} \text{s}^{-1}$				Dry season $\mu\text{molCO}_2\text{m}^{-2} \text{s}^{-1}$			
	Daytime	Nighttime	Daytime peak	Daily total	Daytime	Nighttime	Daytime peak	Daily total
Plateau-Obs	-9.1	5.4	-21.5	-2.4	-8.8	4.5	-21.9	-2.8
Plateau-Sim	-8.5	3.2	-16.7	-3.2	-10.2	2.9	-20.3	-4.2
Valley-Obs	-6.8	4.1	-15.1	-1.8	-6.1	3.9	-19.9	-1.5
Valley-Sim	-7.5	2.6	-14.3	-2.9	-7.8	2.4	-15.3	-3.1

presenting a direct relation with solar radiation fluxes [81]. Our results in Fig. 9 also show this characteristic.

The simulated *NEE* fluxes during daytime indicate higher mean values of *NEE* in the dry season, probably due to higher solar radiation, mainly in the plateau area (about 20% higher compared to wet season), in agreement with literature [82]. In contrast, the observed *NEE* values were 3.3% and 10.2% higher during the wet season in the plateau and valley, respectively. The daytime *NEE* values observed by different authors are different. It was found a higher forest assimilation in the eastern Amazonian site during the dry season [83], opposing to earlier results with higher values in the wet season, related to the rainfall [75]. Although INLAND model does not represent adequately the 2006-year mean seasonality, there was a fair agreement between modeled and observed daily peaks, showing higher values during dry season, mainly in valley area. Lower values of respiration in the valley, in both seasons, may also be associated with a lower decomposition rate of organic matter in this area, due to reduced values of Carbon to Nitrogen ratio (C:N) because of the poor quality of the plant leaves [1]. This can be partially explained by the increased air humidity that favors intense organic matter decomposition by microorganisms [84]. In addition, during the wet season, a greater cloudiness and humidity is observed in the atmosphere, contributing to a lower loss of longwave radiation and less cooling on vegetation canopy. Thence, atmospheric turbulence increases favoring vertical transport and forest-borne CO₂ mixing, both in the plateau and valley areas, during the wet season [31, 85]. Other studies have also found higher respiration values during the wet season [86, 87].

The underestimation of fluxes during dry season was also found by other study in the same area [82]. It is due to the overestimated *NEE* value obtained by the eddy covariance method, observed since the first tests performed using this methodology [88]. This method underestimates CO₂ flux under stable atmospheric conditions during the night Miller et al. [86], when CO₂ flow is characterized by autotrophic respiration and the decomposition of organic material from soil. CO₂ drainage from high (plateau) to low (valley) areas also contributes to the forest CO₂ flow underestimation at night, as at K34 tower site [89, 90].

The observed mid-day dip in *NEE* in the valley is not reproduced in the simulation. The dip can be attributed

to systematic foggy conditions that reduce incoming solar radiation and therefore photosynthesis. This is one of the reasons for lower values of *R*² found in the valley area, especially during the dry season (0.55), when compared to the wet season (0.63) (Table 6). The *R*² values in the plateau (wet = 0.76; dry = 0.66) are higher than those found by other authors (wet = 0.54; dry = 0.41) in the same study area [45, 82]. On the other hand, the *RMSE* values of the two areas were similar. The mean values shown in Table 5 are comparable in magnitude to those reported in the literature, as 4.2 μmol m⁻² s⁻¹, in the plateau area [45]. The discrepancy between the observed and simulated *NEE* values is higher around the hours when the forest changes its physiological activity from respiration to photosynthesis and vice versa. This shows the need for further tuning of floristic, hydrological and soil parameters in the model.

4 Summary and concluding remarks

This study shows the importance of incorporating the diversity of elements that compose the landscape in tropical forests such as vegetation characteristics, pedology and hydrological dynamics into terrestrial surface models. These elements are strongly associated with the local topographic heterogeneity (Fig. 2). The identification and quantification of these elements on a fine spatial scale were essential for the INLAND model, with a lump aquifer model included in it, to capture the main differences related to energy, water and carbon balances between two different environments along a topographic gradient in central Amazon region. The INLAND model with default parameters produced large errors in the simulations of the soil moisture (Fig. 5) and consequently in the hydrological cycle.

The simulated Latent heat flux (*LE*) was higher on the plateau than in the valley (Fig. 8c, d), in both seasons. The dry season *LE* is higher than the wet season *LE* both in the valley and on the plateau. In general, *LE* is several times greater than *H*, meaning that a substantial part of the net radiation *R_n* is expended for evapotranspiration (*ET*) (85% on the plateau and 76% in the valley) and a small part of energy is transferred by the forest directly to the atmosphere as sensible heat (*H*). In the dry season the proportion of *H* increases somewhat, at both valley and plateau sites.

Table 6 Performance of the INLAND model for the representation of the net ecosystem exchange (*NEE*) during 2006, from hourly data

	Plateau		Valley	
	Wet season	Dry season	Wet season	Dry season
<i>RMSE</i> (μmol CO ₂ m ⁻² s ⁻¹)	6.6	7.2	6.4	7.5
Bias (μmol CO ₂ m ⁻² s ⁻¹)	-0.7	-1.5	-0.8	-1.7
<i>R</i> ² (Dimensionless)	0.76	0.66	0.63	0.55

The present study, with floristic, topographic, hydrological and atmospheric parameters tuned to suit the tropical forest environment, simulated the fluxes and their seasonal and diurnal variabilities satisfactorily.

The inclusion of a lumped unconfined aquifer model proved essential to adequately simulate the water balance in the valley environment, highlighting that the valley presents water and soil dynamics distinct from the plateau. The model reasonably reproduced ($R^2 = 0.64$ and 0.62) the temporal variability (seasonal as well as interannual) of the water table depth in the valley (Table 1). The simulations showed that the surface runoff (R_s) in the valley and on the plateau are approximately 25% and 3%, respectively, of the precipitation. The surface models are usually parameterized based on plateau data only [91]. Our results indicate that previous results might be overestimating ET by 8–16%.

In general, NEE flux (Fig. 9) is higher on the plateau during both wet and dry seasons. NEE in the valley is 26% and 9% less than over the plateau during the dry and wet seasons, respectively, showing heterogeneity in photosynthetic activity. In spite of some deficiencies in the simulations, the model results reproduced many important observed characteristics, with better representation than the results reported in earlier studies. Higher agreement (R^2) between the simulations and the observation of NEE than in the experiments of earlier authors was an encouraging factor.

In this study we obtained an understanding of the differences between valley and plateau forests, both by examining the observational data and data simulated by INLAND model. One interesting example is the reduction (or dip) of net radiation (R_n , Fig. 8a) and net ecosystem exchange or CO_2 emission fluxes (Fig. 9a) at the valley site around 11 LT and their re-intensification after an hour or two. This feature is not observed at the plateau site. However, this feature is not captured by the model. The mesoscale and small scale dynamics of the surface flow and the formation of clouds and/or fog in the valley at this time of the day in the wet season should make an interesting topic for research.

The results of this study clearly show spatial heterogeneity of hydrological, biophysical and energy exchange processes which should be taken into account in climate models used for simulating future scenarios. Furthermore, the results serve to validate the version of INLAND model in a typical tropical forest ecosystem. The next major challenge is to develop a land surface model integrated with a subgrid scale variability scheme that allows explicit consideration of the typical processes of each of the environments within the Amazon ecosystem (plateau, slope and valley). This grid refinement can contribute to reduction of uncertainties within the Earth System integrated models in

future climatic scenarios. In addition, the modeling of forest ecosystems response and resilience to climate change can be improved by including the diversity of the landscape functionality.

Studies similar to this at contrasting landscapes such as forest and adjacent deforested areas, and inundated and nearby dry land areas, are capable of showing effects of heterogeneities in the Amazon Basin. These studies contribute to more accurate understanding of energy fluxes and carbon emission estimations in critical areas such as the Amazon rainforest, useful for mitigation strategies tackling the impacts of anthropogenic-induced climate change on the natural ecosystems.

The availability of an appropriate set of soil parameters at deeper layers validated with observed data is important for future model calibrations, especially for heterogeneous landscapes at finer scales.

Acknowledgements The authors would like to thank all support and patience from Dr. Bart Kruijt, Dr. Martin Hodnett and M.Sc. Diogo Amore.

Funding This work was supported by the São Paulo Research Foundation (FAPESP) Grant Number 2017/22269-2. The first author was funded by The National Council of Scientific and Technological Development (CNPq) and National Coordination for High Level Education and Training (CAPES). The second author was supported by CNPq Grant Number 314780/2020-3. The fourth author was supported by Grant Number 2308.019802/2018-7, PVNS (National Senior Visiting Professor) program by CAPES in Brazil and CNPq in Brazil for research Grant number PQ 306595/2013-3.

Data availability The datasets generated and/or analyzed during the current study are not publicly available, because part of them was generated during the PdD from one of the co-authors and other part is from the Large Scale Experiment of the Biosphere-Atmosphere in Amazonia-LBA project. They may be available from corresponding author on reasonable request.

Declarations

Conflict of interest The authors declare that the research was conducted in the absence of any commercial or financial relationships that could be construed as a potential conflict of interest.

Open Access This article is licensed under a Creative Commons Attribution 4.0 International License, which permits use, sharing, adaptation, distribution and reproduction in any medium or format, as long as you give appropriate credit to the original author(s) and the source, provide a link to the Creative Commons licence, and indicate if changes were made. The images or other third party material in this article are included in the article's Creative Commons licence, unless indicated otherwise in a credit line to the material. If material is not included in the article's Creative Commons licence and your intended use is not permitted by statutory regulation or exceeds the permitted use, you will need to obtain permission directly from the copyright holder. To view a copy of this licence, visit <http://creativecommons.org/licenses/by/4.0/>.

References

1. Luizão RCC, Luizão FJ, Paiva RQ, Monteiro TF, Souza LS, Kruijt B (2004) Variation of carbon and nitrogen cycling processes along a topographic gradient in a central Amazonian forest. *Glob Change Biol* 22:592–600. <https://doi.org/10.1111/j.1529-8817.2003.00757.x>
2. Waterloo MJ, Oliveira SM, Drucker DP, Nobre AD, Cuartas LA, Hodnett MG, Langedijk I, Jans WWP, Tomasella J, de Araújo AC, Pimentel TP, Múnera JC (2006) Export of organic carbon in runoff from an Amazonian blackwater catchment. *Hidrol Processes* 20:2581–2597. <https://doi.org/10.1002/hyp.6217>
3. Tomasella J, Hodnett MG, Cuartas LA, Nobre AD, Waterloo J, Oliveira SM (2008) The water balance of an Amazonia micro-catchment: the effect of interannual variability of rainfall on hydrological behaviour. *Hydrol Process* 22:2133–2147. <https://doi.org/10.1002/hyp.6813>
4. Cuartas LA, Tomasella J, Nobre AD, Nobre CA, Hodnett MG, Waterloo JM, de Oliveira SM, von Randow RC, Trancoso R, Ferreira M (2012) Distributed hydrological modeling of a micro-scale rainforest watershed in Amazonia: model evaluation and advances in calibration using the new HAND terrain model. *J Hydrol* 462(463):15–27. <https://doi.org/10.1016/j.jhydrol.2011.12.047>
5. Fisher RA, Williams M, Ruivo ML, De Costa AL, Meir P (2008) Evaluating climatic and soil water controls on evapotranspiration at two Amazonian rainforest sites. *Agric For Meteorol* 148(6–7):850–861
6. Dixon RK, Brown S, Houghton RA, Solomon AM, Trexler MC, Wisniewski J (1994) Carbon pools and flux of global forest ecosystems. *Science* 263(5144):185–190
7. Laurence WFD, Cochrane MA, Berger S, Fearnside PM, Delamonica P, Barber C, D'Angelo S, Fernandes T (2001) The future of the Brazilian Amazon. *Science* 291(5503):438–439
8. Nobre AD, Cuartas LA, Hodnett MG, Rennó CD, Rodrigues G, Silveira A, Waterloo M, Saleska S (2011) Height above the nearest drainage—a hydrologically relevant new terrain model. *J Hydrol* 404:13–29. <https://doi.org/10.1016/j.jhydrol.2011.03.051>
9. Hodnett MG, Vendrame I, Marques-Filho OA, Oyama MD, Tomasella J (1997a) Soil water storage and groundwater behavior in a catenary sequence beneath forest in central Amazonia. Comparisons between plateau, slope and valley floor. *Hydrol Earth Syst Sci* 1:265–277. <https://doi.org/10.5194/hess-1-265-1997>
10. Hodnett MG, Vendrame I, Oyama MD, Marques-Filho AO, Tomasella J (1997) Soil water storage and groundwater behaviour in a catenary sequence beneath forest in central Amazonia flood-plain water table behaviour and implications for stream flow generation. *Hydrol Earth Syst Sci* 1:279–290. <https://doi.org/10.5194/hess-1-279>
11. Brito JM (2010). Estrutura e composição florística de uma floresta de baixo de terra firme da Reserva Adolpho Ducke, Amazônia Central. 2010.78 p. Tese de Mestrado (Mestrado em Botânica), Instituto Nacional de Pesquisas da Amazônia (INPA), Manaus.
12. Pezeshki SR, DeLaune RD (2012) Soil oxidation-reduction in wetlands and its impact on plant functioning. *Biology* 1:196–221. <https://doi.org/10.3390/biology1020196>
13. Li S, Goodwin S, Pezeshki SR (2007) Photosynthetic gene expression in black willow under various soil moisture regimes. *Biol Plant* 51(3):593–596
14. Broedel E, Tomasella J, Cândido LA, Von Randow V (2017) Deep soil water dynamics in an undisturbed primary forest in central Amazonia: differences between normal years and the 2005 drought. *Hydrol Process*. <https://doi.org/10.1002/hyp.11143>
15. Tomasella J, Hodnett MG (1996) Soil hydraulic properties and van Genuchten parameters for an oxisol under pasture in central Amazonia. In: Gash JHC, Nobre CA, Roberts JM, Victoria RL (eds) Amazonian deforestation and climate. Wiley, West Sussex, pp 101–124
16. Dickinson RE, Henderson-Sellers A, Kennedy PJ, Wilson MF (1986) Biosphere-atmosphere transfer scheme (BATS) for the NCAR community climate model. National Center for Atmospheric Research, Colorado, Boulder, p 100
17. Sellers PJ, Mintz Y, Sud YC, Dalcher A (1986) A simple biosphere model (SiB) for use within general circulation models. *J Atmos Sci* 43(6):505–531
18. Noilhan J, Planton S (1989) A simple parameterization of land surface processes for meteorological models. *Mon Weather Rev* 117(3):536–549
19. Verseghy DL (1991) CLASS—a Canadian land surface scheme for GCMs, I. Soil model. *Int J Climatol* 11(4):111–133
20. Foley JA, Prentice IC, Ramankutty N, Levis S, Pollard D, Sitch S, Haxeltine A (1996) An integrated biosphere model of land surface processes, terrestrial carbon balance, and vegetation dynamics. *Global Biogeochem Cycles* 10:603–628. <https://doi.org/10.1029/96GB02692>
21. Dai Y, Zeng X, Dickinson RE, Baker I, Bonan GB, Bosilovich MG, Denning AS et al (2003) The common land model. *Bull Am Meteorol Soc* 84(8):1013–1023
22. Blyth EM, Best M, Cox P, Essery R, Boucher O et al. (2006) JULES: a new community land surface model. IGBP newsletter, vol. 6, p. 9–11.
23. Maquin M, Mouche E, Mügler C, Ducharme A (2015) A water-table, soil, vegetation column model to predict catchment hydrology. American Geophysical Union, Fall Meeting
24. Alvares CA, Stape JL, Sentelhas PC, Gonçalves JLM, Sparovek G (2014) Köppen's climate classification map for Brazil. *Meteorol Z* 22(6):711–728. <https://doi.org/10.1127/0941-2948/2013/0507>
25. Leopoldo PR, Franken W, Salati E, Ribeiro MNG (1987) Towards a water balance in Central Amazonian region. *Experientia* 43:222–233. <https://doi.org/10.1007/BF01945545>
26. Oliveira AN, Amaral IL, Nobre AD, Couto LB, Sato RM, Santos JL, Ramos J (2002) Composição e diversidade florística de uma floresta ombrófila densa de terra firme na Amazônia central, Amazonas, Brasil. II LBA Scientific Conference, Manaus. pp 42.
27. Chauvel A, Lucas Y, Boulet R (1987) On the genesis of the soil mantle of the region of Manaus, central Amazonia, Brazil. *Experientia* 43:234–241
28. Araújo AC, Nobre AD, Kruijt B, Elbers JA, Dallarosa R, Stefani P, Von Randow C, Manzi AO, Culf AD, Gash JHC, Valentini R, Kabat P (2002) Comparative measurements of carbon dioxide fluxes from two nearby towers in a central Amazonian rain forest: the Manaus LBA site. *J Geophys Res* 107:1–20. <https://doi.org/10.1029/2001JD000676>
29. Cuartas LA, Tomasella J, Nobre AD, Hodnett MG, Waterloo MJ, Munera JC (2007) Interception water-partitioning dynamics for a pristine rainforest in Central Amazonia: marked differences between normal and dry years. *Agric For Meteorol* 145:69–83. <https://doi.org/10.1016/j.agrformet.2007.04.008>
30. Chambers JQ, Higuchi N, Teixeira LM, dos Santos J, Laurence SG, Trumbore SE (2004) Response of tree biomass and wood litter to disturbance in a central amazon forest. *Oecologia* 141:596–611. <https://doi.org/10.1007/s00442-004-1676-2>
31. Araújo, AC (2009) Spatial variation of CO₂ fluxes and lateral transport in an area of terra firme forest in Central Amazonia. Tese de doutorado (Doutorado em Ciências Geoambientais)—Free University of Amsterdam, Holanda, p 158
32. Kucharik CJ, Foley JA, Delire C, Fisher VA, Coe MT, Lenters JD, Young-Molling C, Ramankutty N, Norman JM, Gower ST (2000) Testing the performance of a dynamic global ecosystem model:

- water balance, carbon balance, and vegetation structure. *Glob Biogeochem Cycles* 14:795–826. <https://doi.org/10.1029/1999GB001138>
33. Anderson A, Curtas LA, Coe MT, Von Randow C, Castanho A, Ovando A, Nobre AD, Koumrouyan A, Sampaio G, Costa MH (2018) Coupling the terrestrial hydrology model with biogeochemistry to the integrated LAND surface model: Amazon Basin applications. *Hydrol Sci J* 63(13–14):1954–1966
 34. Tourigny, E (2014) Multi-scale fire modeling in the neotropics: coupling a land surface model a to high resolution fire spread model, considering land cover heterogeneity. Tese de doutorado (Doutorado em Meteorologia)—Instituto Nacional de Pesquisas Espaciais (INPE), São Jose dos Campos, São Paulo.
 35. Pollard D, Thompson SL (1995) Use of a land-surface-transfer scheme (LSX) in a global climate model: the response to doubling stomatal resistance. *Glob Planet Change* 10:129–161. [https://doi.org/10.1016/0921-8181\(94\)00023-7](https://doi.org/10.1016/0921-8181(94)00023-7)
 36. Yeh PJF, Eltahir EAB (2005) Representation of water table dynamics in a land surface scheme: model development. *J Climatol* 18:1861–1880. <https://doi.org/10.1175/JCLI3330.1>
 37. Yeh PJF, Eltahir EAB (2005) Representation of water table dynamics in a land surface scheme: subgrid variability. *J Climatol* 18:1881–1901. <https://doi.org/10.1175/JCLI3331.1>
 38. Johnson, A.I. (1967) Specific yield compilation of specific yields for various materials. U.S. Geological. Survey., Water Supply Papers, 1662-D, pp 74.
 39. Lyne, V. & Hollick, M. (1979) “Stochastic time variable rainfall-runoff modelling”, Proceedings of the Hydrology and Water Resources Symposium, Perth, 10–12 September, Institution of Engineers National Conference Publication, No. 79/10, pp. 89–92.
 40. Nathan RJ, McMahon T (1990) Evaluation of automated techniques for baseflow and recession analyses. *Water Resour Res* 26(7):1465–1473. <https://doi.org/10.1029/WR026i007p01465>
 41. Arnold JG, Allen PM (1999) Automated methods for estimating baseflow and ground water recharge from streamflow records. *J Am Water Resour Assoc* 35(2):411–424. <https://doi.org/10.1111/j.1752-1688.1999.tb03599.x>
 42. Furey PR, Grupta VK (2001) A physically based filters for baseflow separation from streamflow time series. *Water Resour Res* 37(11):2709–2722. <https://doi.org/10.1029/2001WR000243>
 43. Lo MH, Yeh PJF, Famiglietti JS (2008) Constraining water table depth simulations in a land surface model using estimated baseflow. *Adv Water Resour* 31(12):1552–1564. <https://doi.org/10.1016/j.advwatres.2008.06.007>
 44. Feddes RA, Kowalik PJ, Zaradny H (1978) Simulation of field water use and crop yield, Simulation monographs. PUDOC, Wageningen, The Netherlands, p 189
 45. Imbuzeiro HMA (2005) Calibração do modelo IBIS na floresta amazônica usando múltiplos sítios. Dissertação (Mestrado em Meteorologia Agrícola)—Universidade Federal de Viçosa, Viçosa, Minas Gerais, pp 92.
 46. Nobre AD (1989) Relação entre Matéria Orgânica e Mineral de uma toposequência Latossolo-Podzol e a Cobertura de Floresta Tropical Úmida na Bacia do Rio Curiaú, Amazônia Central. Dissertação de Mestrado INPA-FUA, Manaus, Amazônia. p 133.
 47. Ranzani G (1980) Identificação e caracterização de alguns solos da Estação Experimental de Silvicultura Tropical do INPA. *Acta Amazônica* 10:7–41
 48. Pinheiro TF (2007) Caracterização e estimativa de biomassa em fitofisionomias de Terra-firme da Amazônia Central por inventário florístico e por textura de imagens simulação do MAPSAR (Multi-Application Purpose SAR). Dissertação (mestrado em Sensoriamento Remoto) - Instituto Nacional de Pesquisas Espaciais (INPE), São José dos Campos. p 111
 49. Ribeiro, J. E. L. S., Hopkins, M. J. G., Vicentini, A., Sothers, C. A., Costa, M. A. S., Brito, J. M., Souza, M. A. D., Martins, L. H. P., Lohmann, L. G., Assunção, P. A. C. L., Pereira, E. C., Silva, C. F., Mesquita, M. R., Procópio, L. C. (1999) Flora da Reserva Ducke: Guia de identificação das plantas vasculares de uma floresta de terra firme na Amazônia Central. Manaus, INPA. pp 816.
 50. Oliveira AN, Amaral IL (2004) Florística e fitossociologia de uma floresta de vertente na Amazônia Central, Amazonas, Brasil. *Acta Amazônica* 34(1):21–34. <https://doi.org/10.1590/S0044-59672004000100004>
 51. Ferreira SJF, Luizão FJ, Mello-Ivo W, Ross SM, Biot Y (2002) Propriedades físicas do solo após extração seletiva de madeira na Amazônia central. *Acta Amazon* 32(3):449–466
 52. Marques, J. D. O (2009) Influência de atributos físicos e hídricos do solo na dinâmica do carbono orgânico sob diferentes coberturas vegetais na Amazônia Central. Tese de doutorado (Doutorado em Ecologia)—Instituto Nacional de Pesquisas da Amazônia/Universidade Federal da Amazônia (INPA/UFAM), Manaus, p 277.
 53. Hodnett MG, Tomasella J (2002) Marked differences between van Genuchten soil water-retention parameters for temperate and tropical soils: a new water-retention pedotransfer function developed for tropical soils. *Geoderma* 108:155–180
 54. Campbell GS, Norman JM (1998) An Introduction to environmental biophysics, 2nd edn. Springer, New York, p 286. <https://doi.org/10.1007/978-1-4612-1626-1>
 55. Verhoef A, Egea G (2014) Modeling plant transpiration under limited soil water: comparison of different plant and soil 25 hydraulic parameterizations and preliminary implications for their use in land surface models. *Agric For Meteorol* 191:22–32. <https://doi.org/10.1016/j.agrformet.2014.02.009>
 56. Ambrose RB, Roesch SE (1982) Dynamic estuary model performance. *J Environ Eng Div* 108(1):51–71
 57. Fan Y, Miguez-Macho G (2010) Potential groundwater contribution to Amazon dry-season evapotranspiration. *Hydrol Earth Syst Sci* 14:2039–2056. <https://doi.org/10.5194/hess-14-2039-2010>
 58. Nortcliff S, Thornes JB (1981) Seasonal variations in the hydrology of a small forested catchment near Manaus, Amazonas, and the implications for its management. In: Lal R, Russel EW (eds) Tropical agricultural hydrology. Wiley, New York, USA
 59. Negrón-Juárez R, Ferreira JF, Mota MC, Faybishenko B, Monteiro MT, Candido LA, Ribeiro RP, Oliveira RC, Araújo AC, Warren JM, Newman BD, Gimenez BO, Varadarajan C, Agarwal D, Borma L, Tomasella J, Higuchi N, Chambers JQ (2020) Calibration, measurement, and characterization of soil moisture dynamics in a central Amazonian tropical forest. *Vadose Zone J*. <https://doi.org/10.1002/vzj2.20070>
 60. Von Randow RCS, Tomasella J, Von Randow C, Araújo AC, Manzi AO (2020) Evapotranspiration and gross primary productivity of secondary vegetation in Amazonia inferred by eddy covariance. *Agric For Meteorol* 294:1141
 61. Massman WJ, Lee X (2002) Eddy covariance flux corrections and uncertainties in long-term studies of carbon and energy exchanges. *Agric For Meteorol* 113(1–4):121–144
 62. Aubinet M, Heinesch B, Longdoz B (2002) Estimation of the carbon sequestration by a heterogeneous forest: night flux corrections, heterogeneity of the site and inter-annual variability. *Glob Change Biol* 8(11):1053–1071
 63. Malhi Y, Phillips OL, Baker T, Wright J, Almeida S, Arroyo L, Frederiksen T, Grace J, Higuchi N, Kileen T, Laurance WF, Leão C, Meir P, Monteagudo A, Neill D, Núñez Vargas P, Panfil SN, Patiño S, Pitman N, Quesada CA, Rudas-LI A, Salomão R, Saleska S, Silva N, Silveira M, Sombroek WG, Valencia R, Vásquez Martínez R, Vieira ICG, Vicenti B (2002) An international network to understand the biomass and dynamics of Amazonian forests (RAINFOR). *J Veg*

- Sci 13:439–450. <https://doi.org/10.1111/j.1654-1103.2002.tb02068.x>
64. Von Randow C, Manzi AO, Kruijt B, de Oliveira PJ, Zanchi FB, Silva RL, Hodnett MG, Gash JHC, Elbers JA, Waterloo MJ, Cardoso FL, Kabat P (2004) Comparative measurements and seasonal variations in energy and carbon exchange over forest and pasture in southwest Amazonia. *Theor Appl Climatol*. <https://doi.org/10.1007/s00704-004-0041-z>
65. Rocha HR, Goulden ML, Miller SD, Menton MC, Pinto LDVO, Freitas HC, Figueira AMS (2004) Seasonality of water and heat fluxes over a tropical forest in eastern Amazonia. *Ecol Appl* 14(4):S22–S32
66. Wilson K, Goldstein A, Falge E, Aubinet M, Baldocchi D, Berbigier P, Bernhofer C, Ceulemans R, Dolman H, Field C, Grelle A, Ibrom A, Law BE, Kowalski A, Meyers T, Moncrieff J, Monson R, Oechel W, Tenhunen RV, Shashi V (2002) Energy balance closure at FLUXNET sites. *Agric For Meteorol* 113(1–4):223–243. [https://doi.org/10.1016/S0168-1923\(02\)00109-0](https://doi.org/10.1016/S0168-1923(02)00109-0)
67. Martínez-Cob A, Suvocarev K (2015) Uncertainty due to hygrometer sensor in eddy covariance latent heat flux measurements. *Agric For Meteorol* 200:92–96. <https://doi.org/10.1016/j.agrfor.2014.09.021>
68. Van Dijk AIJM, Gash JH, Van Gorsel E, Blanken PD, Cescatti A, Emmel C, Gielen B, Harman IN, Kiely G, Merbold L, Montagnani L, Moors E, Sottocornola M, Varlagin A, Williams CA, Wohlfahrt G (2015) Rainfall interception and the coupled surface water and energy balance. *Agric For Meteorol* 214–215:402–415
69. Luizão FJ (1989) Litter production and mineral element input to the forest floor in a central Amazonian forest. *J Geol* 19:407–417. <https://doi.org/10.1007/BF00176910>
70. Leopoldo PR, Franken WK, Villa Nova NA (1995) Real evapotranspiration and transpiration through a tropical rain forest in central Amazonia as estimated by the water balance method. *For Ecol Manag* 73(1–3):185–195
71. Germer S, Neill C, Vetter T, Chaves J, Krusche AV, Elsenbeer H (2009) Implications of long-term land-use change for the hydrology and solute budgets of small catchments in Amazonia. *J Hydrol* 364(3–4):349–363. <https://doi.org/10.1016/j.jhydrol.2008.11.013>
72. Moraes JM, Schuler AE, Dunne T, Figueiredo RO, Victoria R (2006) Water storage and runoff processes in plinthic soils under forest and pasture in eastern Amazonia. *Hydrol Process* 20:2509–2526. <https://doi.org/10.1002/hyp.6213>
73. Oliveira MBL (2010) Estudo das trocas de energia sobre a floresta amazônica. 2010. 144 p. Tese de Doutorado (Doutorado em Ciências de Florestas Tropicais)—Instituto Nacional de Pesquisas da Amazônia (INPA), Amazônia, p 144
74. Leitão MMVBR (1994) Balanço de radiação em três ecossistemas da Floresta Amazônica: Campina, Campinarana e Mata densa. Tese de doutorado (Doutorado em Meteorologia)—Instituto Nacional de Pesquisas Espaciais (INPE), São Jose dos Campos, p 157.
75. Malhi Y, Nobre AD, Grace J, Kruijt B, Pereira MGP, Culf A, Scott S (1998) Carbon dioxide transfer over a Central Amazonian rain forest. *J Geophys Res* 103(24):31593–31612. <https://doi.org/10.1029/98JD02647>
76. Pezeshki SR (2001) Wetland plant responses to soil flooding. *Environ Exp Bot* 46(3):299–312
77. Varejão EVV, Bellato CR, Fontes MPF, Mello JWV (2011) Arsenic and trace metals in river water and sediments from the southeast portion of the Iron Quadrangle, Brazil. *Environ Monit Assess* 172(1):631–642. <https://doi.org/10.1007/s10661-010-1361-3>
78. de Castilho CV, Magnusson WE, de Araújo RNO, Luizão RCC, Luizão FJ, Lima AP, Higuchi N (2006) Variation in aboveground tree life biomass in a central Amazonian forest: effects of soil and topography. *For Ecol Manag* 234:85–96. <https://doi.org/10.1016/j.foreco.2006.06.024>
79. Laurance WFD, Fearnside PM, Laurance SG, Delamonica P, Lovejoy TE, de Merona MR, Chambers QC, Gascon C (1999) Relationship between soils and Amazon forest biomass: a landscape-scale study. *For Ecol Manag* 118(1–3):127–138. [https://doi.org/10.1016/S0378-1127\(98\)00494-0](https://doi.org/10.1016/S0378-1127(98)00494-0)
80. Zanchi FB (2013) Vulnerability to drought and soil carbon exchange of valley forest in Central Amazonia—Brazil. Tese de doutorado (Doutorado em Ciências Geoambientais). Free University of Amsterdam, Holanda, p 186
81. Stjinman J (2015) Sapflow start times in the Asu catchment, Brazil. VU University, Faculty of Earth and Life Sciences, Amsterdam, p 17
82. Assunção, L. (2011) Aplicação do modelo de vegetação dinâmica IBIS às condições de floresta de terra firme na região central da Amazônia. Tese de Mestrado (Mestrado em Clima e Ambiente), Instituto Nacional de Pesquisas da Amazônia/ Universidade do Estado do Amazonas (INPA/UEA), Manaus, p 103.
83. Goulden ML, Miller SD, da Rocha HR, Menton MC, de Freitas HC, Figueira AMES, de Souza CAD (2004) Diel and seasonal patterns of tropical forest CO₂ exchange. *Ecol Appl* 14(4):S42–S54
84. Luizão FJ, Schubart HOR (1987) Litter production and decomposition in a terra-firme forest of Central Amazonia. *Experientia* 43(3):259–265
85. Miller SD, Goulden ML, Menton MC, da Rocha HR, de Freitas HC, Figueira AMES, de Souza CAD (2004) Biometric and micrometeorological measurements of tropical forest carbon balance. *Ecol Appl* 14(4):114–126. <https://doi.org/10.1890/02-6005>
86. Zanchi FB, Meesters AGCA, Waterloo JM, Kruijt B, Kesselmeier J, Luizão FL, Dolman AJ (2014) Soil CO₂ exchange in seven pristine Amazonian rain forest sites in relation to soil temperature. *Agric For Meteorol* 192–193:96–107. <https://doi.org/10.1016/j.agrfor.2014.03.009>
87. Souza, J. S. (2004) Dinâmica espacial e temporal do fluxo de CO₂ do solo em floresta de terra firme na Amazônia Central. Master's thesis, Instituto Nacional de Pesquisas da Amazonia and Universidade Federal do Amazonas Manaus, Amazonas State, Brazil
88. Ohtaki E (1984) Application of an infrared carbon dioxide and humidity instrument to studies of turbulent transport. *Boundary Layer Meteorol* 29:85–107. <https://doi.org/10.1007/BF0011912>
89. Tota J, Fitzjarrald DR, Staebler RM, Sakai RK, Moraes OMM, Acevedo OC, Wofsy SC, Manzi AO (2008) Amazon rain forest sub-canopy flow and the carbon budget: Santarém LBA-ECO site. *J Geophys Res Biogeosci* 113(15):G00B02. <https://doi.org/10.1029/2007JG000597>
90. Araújo AC, Dolman AJ, Waterloo MJ, Gash JHC, Kruijt B, Zanchi FB, Lange JME, Stoevelaar R, Manzi AO, Nobre AD, Lootens RN, Backer J (2010) The 45spatial variability of CO₂ storage and the interpretation of eddy covariance fluxes in central Amazonia. *Agric For Meteorol* 150:226–237. <https://doi.org/10.1016/j.agrfor.2009.11.005>
91. Harris PP, Huntingford C, Gash JHC, Hodnett M, Cox PM, Malhi Y, Araujo AC (2004) Calibration of a land-surface model using data from primary forest sites in Amazonia. *Theor Appl Climatol* 78(13):27–45

Publisher's Note Springer Nature remains neutral with regard to jurisdictional claims in published maps and institutional affiliations.